

# The NNLO soft function for the pair invariant mass distribution of boosted top quarks

ANDREA FERROGLIA<sup>a</sup>, BEN D. PECJAK<sup>b</sup>, AND LI LIN YANG<sup>c</sup>

<sup>a</sup>*New York City College of Technology, 300 Jay Street  
Brooklyn, NY 11201, USA*

<sup>b</sup>*Institut für Physik (THEP), Johannes Gutenberg-Universität  
D-55099 Mainz, Germany*

<sup>c</sup>*Institute for Theoretical Physics, University of Zürich  
CH-8057 Zürich, Switzerland*

## Abstract

At high values of the pair invariant mass the differential cross section for top-quark pair production at hadron colliders factorizes into soft, hard, and fragmentation functions. In this paper we calculate the next-to-next-to-leading-order (NNLO) corrections to the soft function appearing in this factorization formula, thus providing the final piece needed to evaluate at NNLO the differential cross section in the virtual plus soft approximation in the large invariant-mass limit. Technically, this amounts to evaluating the vacuum expectation value of a soft Wilson loop operator built out of light-like Wilson lines for each of the four partons participating in the hard scattering process, with a certain constraint on the total energy of the soft radiation. Our result turns out to be surprisingly simple, because in the sum of all graphs the three and four parton contributions multiply color structures whose coefficients are governed by the non-abelian exponentiation theorem.

# 1 Introduction

The pair invariant mass distribution is an important observable in top-quark pair production at hadron colliders. Especially interesting is the high invariant-mass region of the distribution, which could potentially be distorted by new physics without disturbing the good agreement between Standard Model and experiment for the total cross section. The phenomenological importance of this distribution motivates special attention to its calculation in the Standard Model.

Theory predictions of the invariant mass distribution typically rely on the next-to-leading order (NLO) computations of two-particle inclusive cross sections carried out in [1], supplemented with soft gluon resummation at the level of next-to-leading-logarithmic (NLL) [2,3] or more recently next-to-next-to-leading-logarithmic (NNLL) [4] accuracy. The resummed calculations take into account higher-order logarithmic plus-distribution corrections related to gluon emission in the soft limit  $z = M^2/\hat{s} \rightarrow 1$ , with  $M$  the pair invariant mass and  $\sqrt{\hat{s}}$  the partonic center-of-mass energy. However, except at restrictively high values of the invariant mass where  $\tau = M^2/s \rightarrow 1$ , with  $\sqrt{s}$  the hadronic center-of-mass energy, the dominance of these logarithmic corrections over  $\delta(1-z)$  corrections relies on the mechanism of dynamical threshold enhancement studied in [5–8]. In fact, numerical comparisons of exact NLO results with the leading terms in the soft limit show good agreement only if the delta-function terms are included to achieve a full virtual plus soft approximation [9]. Starting at NNLO, such a virtual plus soft approximation is not achieved through expansions of NNLL resummation formulas alone, and even though the delta-function contributions are formally N<sup>3</sup>LL corrections the only way to know their size for certain is to calculate them.<sup>1</sup> Moreover, the soft gluon resummation mentioned above uses the generic counting  $m_t \sim M$  for the top-quark mass, whereas at truly high values of the invariant mass the counting  $m_t \ll M$  should be used, and resummation must also take into account logarithms of the ratio  $m_t/M$ .

In a recent paper [12], we have set up a factorization formalism appropriate for the invariant-mass distribution in the simultaneous soft and small-mass ( $m_t \ll M$ ) limit. Schematically, the factorization is of the form

$$d\hat{\sigma} = \text{Tr} [\mathbf{HS}] \otimes D \otimes D + \mathcal{O}(1-z) + \mathcal{O}\left(\frac{m_t}{M}\right). \quad (1)$$

The hard function  $\mathbf{H}$  and the soft function  $\mathbf{S}$  are matrices in the space of color-singlet operators for  $(q\bar{q}, gg) \rightarrow t\bar{t}$  scattering, evaluated with  $m_t = 0$ , while the  $D$  are perturbative heavy-quark fragmentation functions containing the dependence on  $m_t$ . Given this form of factorization, one can derive and solve renormalization-group (RG) equations for the individual functions to resum soft logarithms as well as those depending on  $m_t/M$ . Just as importantly, the individual functions appearing in (1) are much easier to calculate in fixed-order perturbation theory than the hard and soft functions needed for soft gluon resummation for generic  $m_t$ . In fact, the fragmentation function is completely known to NNLO accuracy [13], and the higher-order virtual corrections to two-to-two scattering needed to extract the contribution of the NNLO

---

<sup>1</sup>The delta-function terms and also non-singular terms in the soft limit would be included in a full NNLO calculation, but current NNLO results are limited to certain  $q\bar{q}$ -initiated contributions to the total cross section [10,11].

hard function to the differential cross section are also known [14–18]. The only missing piece needed to obtain at NNLO a full soft plus virtual approximation in the limit of large invariant mass is the soft function  $\mathcal{S}$ . The calculation of this soft function to NNLO is the subject of this paper.

Our main motivation for this calculation is its eventual impact on the phenomenology of top-quark pair production. However, we consider it an interesting problem even apart from this. The soft function we deal with here is related to double real emission corrections to massless two-to-two scattering, and at the technical level is defined as the vacuum expectation value of a Wilson loop built out of four light-like Wilson lines. While a number of soft functions have been calculated at NNLO in the literature, these all involve either two [19–25] or three [26] Wilson lines. Compared to those cases, the four-Wilson-line soft function is characterized by the added conceptual complication of a non-trivial matrix structure in color space. One might also expect it to be computationally much more complicated because, unlike the case studied in [26], graphs with attachments of gluons to three Wilson lines do not vanish and in general are complicated functions of two non-trivial scalar products. However, we find that in the sum of all diagrams such three-parton contributions multiply a color structure whose coefficient is determined by the non-abelian exponentiation theorem [27, 28]. In particular, the bare function does not contain a three parton term with the antisymmetric color structure of a three-gluon vertex. This is an expected result for the IR divergent pieces of the bare function, as a consequence of the form of the RG equation derived in [12]. In particular, the momentum dependence in the anomalous dimension governing this RG equation is inherited from the anomalous dimension for scattering amplitudes and is of the dipole type at least to NNLO, which follows from results in [29, 30] (and may even be true to all orders, as conjectured in [31–33]). For the IR finite pieces it is perhaps slightly unexpected that the three parton terms are determined by non-abelian exponentiation, but this is nonetheless the case due to cancellations among certain diagrams.

The remainder of this paper is organized as follows. First, in Section 2 we give the precise definition of the soft function calculated in this paper and we also review the NLO calculation from [12], using it as a means of introducing some of the formalism related to the color-space matrix structure. Then, in Section 3 we present an expression for the bare NNLO soft function as a sum over legs and give explicit results for the component integrals and matrix structures appearing in this sum. We also describe cross checks, both with the two-Wilson-line integrals calculated in [24] and with the non-abelian exponentiation theorem. Finally, in Section 4, we discuss the renormalization procedure and explain how this provides a further cross check on our result. We conclude in Section 5, relegating several details of the calculation along with the final results for the NNLO soft function to the appendix.

## 2 Definitions and the NLO calculation

We define the soft function for the pair-invariant mass distribution as in [4], adapted to the massless case by replacing time-like velocity vectors by light-like ones [12]. The basic objects

for the soft function are firstly the Wilson lines

$$\mathbf{S}_i(x) = \mathcal{P} \exp \left( ig_s \int_{-\infty}^0 ds n_i \cdot A^a(x + sn_i) \mathbf{T}_i^a \right), \quad (2)$$

where the  $\mathcal{P}$  refers to path ordering, and secondly the Wilson loop built out of these objects,

$$\mathbf{O}_s(x) = [\mathbf{S}_{n_1} \mathbf{S}_{n_2} \mathbf{S}_{n_3} \mathbf{S}_{n_4}](x). \quad (3)$$

We have used the notation of [34, 35], where the bold-face indicates that the objects  $\mathbf{T}_i^a$  are matrices acting on color structures specific to the type of partons participating in the two-to-two scattering process. This notation allows us to describe simultaneously the case where the Wilson lines  $\mathbf{S}_i$  associated with the four partons are in any combination of the fundamental (for quarks) or adjoint (for gluons) representations. In this paper we have in mind applications to top-quark pair production in the soft limit, and so will give results appropriate for  $(q\bar{q}, gg) \rightarrow t\bar{t}$  scattering.

The Wilson-loop operator (3) takes into account the coupling of soft gluons to the external partons within the eikonal approximation. The soft function is related to the contribution of these gluon emissions at the level of the squared amplitude. In [12], it was defined through the Fourier transform of a position-space soft function evaluated in the parton center-of-mass frame. In the present work, we will find it more convenient to work directly with the following momentum-space representation<sup>2</sup>:

$$\mathbf{S}(\omega, t_1/M^2, \mu) = \frac{1}{d_R} \sum_{X_s} \langle 0 | \mathbf{O}_s^\dagger(0) | X_s \rangle \langle X_s | \mathbf{O}_s(0) | 0 \rangle \delta(\omega - (n_1 + n_2) \cdot p_{X_s}), \quad (4)$$

where  $d_R = N$  in the  $q\bar{q}$  channel, and  $d_R = N^2 - 1$  in the  $gg$  channel, with  $N$  the number of colors. As usual,  $X_s$  refers to a final state built up of any number of unobserved soft gluons. It is clear from (4) that the soft function depends on the single dimensionful parameter  $\omega$  (and  $\mu$ , upon renormalization), as well as the scalar products  $n_i \cdot n_j$ . Although the results we give later on can be used to construct the soft function for arbitrary velocity vectors, we have defined it in the natural way for two-to-two scattering. In that case there are only two independent scalar products and thus one non-trivial dimensionless ratio, which we have chosen as  $n_1 \cdot n_3 / n_1 \cdot n_2 = n_2 \cdot n_4 / n_1 \cdot n_2 = -t_1/M^2$ . Our notation is then in direct correspondence with the Mandelstam variables used in [12]. It further implies that  $n_1 \cdot n_4 / n_1 \cdot n_2 = n_2 \cdot n_3 / n_1 \cdot n_2 = 1 + t_1/M^2 \equiv -u_1/M^2$  and  $n_1 \cdot n_2 = n_3 \cdot n_4 = 2$ . In the parton center-of-mass-frame, the delta function constrains the energy of the soft radiation to  $2E_s = \omega$ , and it is an easy matter to show the correspondence with the position-space definition used in [12].

In order to study the higher-order corrections which are the subject of this paper, we define expansion coefficients of the bare soft function in  $d = 4 - 2\epsilon$  dimensions as

$$\mathbf{S}_{\text{bare}} = \mathbf{S}^{(0)} + \left( \frac{Z_\alpha \alpha_s}{4\pi} \right) \mathbf{S}_{\text{bare}}^{(1)} + \left( \frac{Z_\alpha \alpha_s}{4\pi} \right)^2 \mathbf{S}_{\text{bare}}^{(2)} + \dots \quad (5)$$

---

<sup>2</sup>Note that this definition differs from [12] by a factor of  $\sqrt{\hat{s}}$ , which we have chosen to omit here. The Laplace-transformed function in (47), on the other hand, coincides with the one introduced in [12].

In the above equation we have expressed the bare coupling constant  $\alpha_s^{(0)}$  in terms of the renormalized one in the  $\overline{\text{MS}}$  scheme: the relation between the two is  $Z_\alpha \alpha_s \mu^{2\epsilon} = e^{-\epsilon\gamma_E} (4\pi)^\epsilon \alpha_s^{(0)}$  with  $Z_\alpha = 1 - \beta_0 \alpha_s / (4\pi\epsilon)$  and  $\beta_0 = 11/3N - 2/3n_l$ , with  $n_l$  the number of light flavors. The soft function for massless partons was obtained to NLO in [12]. We end this section by reviewing the elements that go into that calculation. This gives us an opportunity to introduce the aspects of the color-space formalism needed in this work, and to extend our previous results to the depth of the  $\epsilon$ -expansion needed for the NNLO calculation.

The color-space formalism provides a means of representing soft gluon emissions from external quarks and gluons in a unified way. The important point for the case at hand is that these soft emissions can mix the possible color-singlet structures appearing in the two-to-two scattering amplitudes. To explain the matrix structure relevant for this mixing, we must first define a color basis for  $(q^{a_1} \bar{q}^{a_2}, g^{a_1} g^{a_2}) \rightarrow t^{a_3} \bar{t}^{a_4}$  scattering, where the  $\{a\}$  label the color indices of the partons with velocity  $n_i$ . We work in the  $s$ -channel singlet-octet basis

$$\begin{aligned} (c_1^{q\bar{q}})_{\{a\}} &= \delta_{a_1 a_2} \delta_{a_3 a_4}, & (c_2^{q\bar{q}})_{\{a\}} &= t_{a_2 a_1}^c t_{a_3 a_4}^c, \\ (c_1^{gg})_{\{a\}} &= \delta^{a_1 a_2} \delta_{a_3 a_4}, & (c_2^{gg})_{\{a\}} &= i f^{a_1 a_2 c} t_{a_3 a_4}^c, & (c_3^{gg})_{\{a\}} &= d^{a_1 a_2 c} t_{a_3 a_4}^c. \end{aligned} \quad (6)$$

We view these structures as basis vectors  $|c_I\rangle$  in the space of color-singlet amplitudes. Inner products in this space are defined through a summation over color indices as

$$\langle c_I | c_J \rangle = \sum_{\{a\}} (c_I)_{a_1 a_2 a_3 a_4}^* (c_J)_{a_1 a_2 a_3 a_4}. \quad (7)$$

This inner product is proportional but not equal to  $\delta_{IJ}$ , so the basis vectors are orthogonal but not orthonormal. The soft function matrix elements are defined as

$$\mathbf{S}_{IJ} = \langle c_I | \mathbf{S} | c_J \rangle. \quad (8)$$

The soft function is thus a two-by-two matrix in the  $q\bar{q}$  channel, and a three-by-three matrix in the  $gg$  channel. At leading order (LO), a short calculation yields the result

$$\mathbf{S}_{q\bar{q}}^{(0)} = \delta(\omega) \begin{pmatrix} N & 0 \\ 0 & \frac{C_F}{2} \end{pmatrix}, \quad \mathbf{S}_{gg}^{(0)} = \delta(\omega) \begin{pmatrix} N & 0 & 0 \\ 0 & \frac{N}{2} & 0 \\ 0 & 0 & \frac{N^2-4}{2N} \end{pmatrix}. \quad (9)$$

At NLO and beyond gluon emissions from eikonal lines are associated with factors of  $\mathbf{T}_i$ . One determines the matrix elements (8) by using a set of rules which dictate how the  $\mathbf{T}_i$  act on the color indices  $\{a\}$  of the color structures (2) and performing the sum over colors indicated in (7). These rules are as follows [34, 35]: if the  $i$ -th parton is a final-state quark or an initial-state anti-quark we set  $(\mathbf{T}_i^c)_{ba} = t_{ba}^c$ , for a final-state anti-quark or an initial-state quark we have  $(\mathbf{T}_i^c)_{ba} = -t_{ab}^c$ , and for a gluon we use  $(\mathbf{T}_i^c)_{ba} = i f^{abc}$ . In (4) there is also a conjugated operator  $\mathbf{O}_s^\dagger$ , which contains conjugated color matrices  $\mathbf{T}_i^{a\dagger}$  acting to the left. However, we can drop the daggers and let them act to the right, using the relation

$$\langle \mathcal{M} | \mathbf{T}_i^{a\dagger} | \mathcal{M}' \rangle = (\mathbf{T}_i^a | \mathcal{M} \rangle)^\dagger | \mathcal{M}' \rangle = | \mathcal{M} \rangle^\dagger (\mathbf{T}_i^a | \mathcal{M}' \rangle) = \langle \mathcal{M} | \mathbf{T}_i^a | \mathcal{M}' \rangle, \quad (10)$$

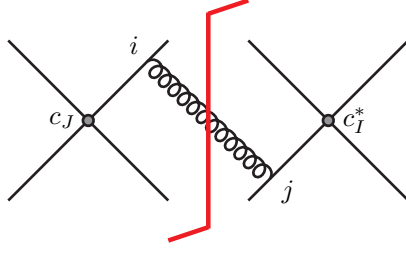


Figure 1: Diagram contributing to the NLO soft function.

with  $|\mathcal{M}\rangle$  and  $|\mathcal{M}'\rangle$  being two arbitrary vectors in color space. This can be easily understood by noting that  $\mathbf{T}_i^a$  is a Hermitian operator. To show explicitly that this relation holds, it is sufficient to work out the case where  $i = 1$  and  $|\mathcal{M}\rangle$  and  $|\mathcal{M}'\rangle$  are two basis vectors  $|a_1, \dots\rangle$  and  $|b_1, \dots\rangle$ . We then have

$$\begin{aligned} (\mathbf{T}_1^c |a_1, \dots\rangle)^\dagger |b_1, \dots\rangle &= ((\mathbf{T}_1^c)_{d_1 a_1} |d_1, \dots\rangle)^\dagger |b_1, \dots\rangle = (\mathbf{T}_1^c)_{d_1 a_1}^* \delta_{b_1 d_1} = (\mathbf{T}_1^c)_{a_1 b_1}, \\ |a_1, \dots\rangle^\dagger (\mathbf{T}_1^c |b_1, \dots\rangle) &= |a_1, \dots\rangle^\dagger ((\mathbf{T}_1^c)_{d_1 b_1} |d_1, \dots\rangle) = (\mathbf{T}_1^c)_{d_1 b_1} \delta_{a_1 d_1} = (\mathbf{T}_1^c)_{a_1 b_1}. \end{aligned}$$

Note also that if there is more than one  $\mathbf{T}$  matrix acting on the same Wilson line, the conjugation reverses their order, e.g.,

$$(\mathbf{T}_i^a \mathbf{T}_i^b |\mathcal{M}\rangle)^\dagger |\mathcal{M}'\rangle = |\mathcal{M}\rangle^\dagger (\mathbf{T}_i^b \mathbf{T}_i^a |\mathcal{M}'\rangle). \quad (11)$$

This is crucial for the cancellations of certain contributions which we will encounter later on.

The formalism is now in place to discuss the NLO calculation. This requires us to evaluate the type of diagram shown in Figure 1 and perform a sum over attachments to the different legs. The diagram represents the connection of gluons to Wilson lines for two distinct particles  $i$  and  $j$ . Diagrams involving virtual corrections or two attachments to the same line are scaleless and vanish in dimensional regularization. To evaluate the diagram we associate each gluon emission with the Feynman rules for eikonal attachments following from (2) and set the cut propagator (for which we use Feynman gauge) on shell with positive energy. This results in an expression proportional to the integral

$$I_1(\omega, a_{ij}) = \int [dk] \frac{n_i \cdot n_j \delta(\omega - n_0 \cdot k)}{n_i \cdot k n_j \cdot k} \equiv \pi^{1-\epsilon} e^{-\epsilon\gamma_E} \omega^{-1-2\epsilon} \bar{I}_1(a_{ij}), \quad (12)$$

where  $[dk] = d^d k \delta(k^2) \theta(k^0)$  and

$$a_{ij} \equiv 1 - \frac{n_0^2 n_i \cdot n_j}{2 n_0 \cdot n_i n_0 \cdot n_j}. \quad (13)$$

For top-quark production, where  $n_0^2 = (n_1 + n_2)^2 = 4$ , we have  $a_{12} = a_{34} = 0$ ,  $a_{13} = a_{24} = -u_1/M^2$ ,  $a_{14} = a_{23} = -t_1/M^2$ . Later on we will describe cross-checks of our result with the simpler NNLO soft functions for Drell-Yan [19] and electroweak boson production at

large  $p_T$  [26]. These involve the same two-Wilson-line integrals but with  $a = 0$  and  $a = 1$  respectively.

The integral in (12) can be parameterized in terms of the gluon energy and an angular integral which is of the type considered long ago in [36]. We have rederived the result using the light-cone coordinate decomposition from [26], which turns out to be especially convenient for the NNLO integrals considered later on. Either way, the result for the stripped integral is

$$\bar{I}_1(a) = \frac{2 e^{\epsilon\gamma_E} \Gamma(-\epsilon)}{\Gamma(1-2\epsilon)} (1-a)^{-\epsilon} {}_2F_1(-\epsilon, -\epsilon, 1-\epsilon, a), \quad (14)$$

which can be expanded in  $\epsilon$  using

$$\begin{aligned} {}_2F_1(-\epsilon, -\epsilon, 1-\epsilon, a) &= 1 + H_2(a)\epsilon^2 + (H_3(a) - H_{2,1}(a))\epsilon^3 \\ &\quad + (H_4(a) - H_{3,1}(a) + H_{2,1,1}(a))\epsilon^4 + \dots \end{aligned} \quad (15)$$

The functions  $H$  indicate Harmonic Polylogarithms<sup>3</sup> (HPLs) [37]. Here and elsewhere in the paper we have used the Mathematica package HypExp [38] in expanding the hypergeometric functions and manipulated the resulting HPLs with the package HPL [39].

We obtain the bare NLO soft function through the following sum over legs:

$$\begin{aligned} \mathbf{S}_{\text{bare}}^{(1)} &= \frac{2}{\omega} \left(\frac{\mu}{\omega}\right)^{2\epsilon} \sum_{\text{legs}} \mathbf{w}_{ij}^{(1)} \bar{I}_1(a_{ij}) \\ &= \frac{4}{\omega} \left(\frac{\mu}{\omega}\right)^{2\epsilon} \left( \mathbf{w}_{12}^{(1)} \bar{I}_1(a_{12}) + \mathbf{w}_{34}^{(1)} \bar{I}_1(a_{12}) + 2\mathbf{w}_{13}^{(1)} \bar{I}_1(a_{13}) + 2\mathbf{w}_{14}^{(1)} \bar{I}_1(a_{14}) \right). \end{aligned} \quad (16)$$

We have taken into account the relations between the  $a_{ij}$  and also the explicit form of the color matrices given below to simplify the sum. The matrix structure in color space is obtained by evaluating the matrix elements of

$$\mathbf{w}_{ij}^{(1)} = -\frac{1}{d_R} \mathbf{T}_i \cdot \mathbf{T}_j, \quad (17)$$

as in (8). Results were given in [4], and we reprint them here for convenience. In the  $q\bar{q}$  channel they read

$$\begin{aligned} \mathbf{w}_{12}^{(1)} = \mathbf{w}_{34}^{(1)} &= \frac{C_F}{4N} \begin{pmatrix} 4N^2 & 0 \\ 0 & -1 \end{pmatrix}, \\ \mathbf{w}_{13}^{(1)} = \mathbf{w}_{24}^{(1)} &= \frac{C_F}{2} \begin{pmatrix} 0 & 1 \\ 1 & 2C_F - \frac{N}{2} \end{pmatrix}, \end{aligned}$$

---

<sup>3</sup>We write the HPLs in the compact notation which eliminates the zeros in the weight vector by adding at the same time one to the absolute value of the previous index to the right; for example  $H_2(a) = H(0, 1; a)$ ,  $H_4(a) = H(0, 0, 0, 1; a)$ ,  $H_{2,1,1}(a) = H(0, 1, 1, 1; a)$ , etc.

$$\mathbf{w}_{14}^{(1)} = \mathbf{w}_{23}^{(1)} = \frac{C_F}{2N} \begin{pmatrix} 0 & -N \\ -N & 1 \end{pmatrix}, \quad (18)$$

while for the  $gg$  channel they are

$$\begin{aligned} \mathbf{w}_{12}^{(1)} &= \frac{1}{4} \begin{pmatrix} 4N^2 & 0 & 0 \\ 0 & N^2 & 0 \\ 0 & 0 & N^2 - 4 \end{pmatrix}, \\ \mathbf{w}_{34}^{(1)} &= \begin{pmatrix} C_F N & 0 & 0 \\ 0 & -\frac{1}{4} & 0 \\ 0 & 0 & -\frac{N^2 - 4}{4N^2} \end{pmatrix}, \\ \mathbf{w}_{13}^{(1)} = \mathbf{w}_{24}^{(1)} &= \frac{1}{8} \begin{pmatrix} 0 & 4N & 0 \\ 4N & N^2 & N^2 - 4 \\ 0 & N^2 - 4 & N^2 - 4 \end{pmatrix}, \\ \mathbf{w}_{14}^{(1)} = \mathbf{w}_{23}^{(1)} &= \frac{1}{8} \begin{pmatrix} 0 & -4N & 0 \\ -4N & N^2 & -(N^2 - 4) \\ 0 & -(N^2 - 4) & N^2 - 4 \end{pmatrix}. \end{aligned} \quad (19)$$

As usual,  $C_F = (N^2 - 1)/2N$  and  $C_A = N$ .

At NLO the renormalized function in the  $\overline{\text{MS}}$  scheme can be obtained from the bare function simply by dropping the poles. More formally, we need to multiply it on both sides by a UV renormalization matrix. We describe the formal procedure in more detail in Section 4, after performing the NNLO calculation in the next section.

### 3 The bare soft function at NNLO

In this section we calculate the bare soft function at NNLO. We find that in the sum of all diagrams the result can be written in the form

$$\begin{aligned} \mathbf{S}_{\text{bare}}^{(2)} &= \frac{4}{\omega} \left( \frac{\mu}{\omega} \right)^{4\epsilon} \sum_{\text{legs}} \left( \sum_{n=2}^7 \mathbf{w}_{ij}^{(n)} \bar{I}_n(a_{ij}) + \mathbf{w}_{ijk}^{(8)} \bar{I}_8(a_{ij}, a_{ik}) + \mathbf{w}_{ijkl}^{(9)} \bar{I}_9(a_{ij}, a_{kl}) \right) \\ &= \frac{4}{\omega} \left( \frac{\mu}{\omega} \right)^{4\epsilon} \left[ 2 \left( \mathbf{w}_{12}^{(1)} + \mathbf{w}_{34}^{(1)} \right) \left( \bar{I}_2(a_{12}) + C_A \bar{I}_6(a_{12}) + C_A \bar{I}_{7,1}(a_{12}) + C_A \bar{I}_{7,2}(a_{12}) \right) \right. \\ &\quad + 4\mathbf{w}_{13}^{(1)} \left( \bar{I}_2(a_{13}) + C_A \bar{I}_6(a_{13}) + C_A \bar{I}_{7,1}(a_{13}) + C_A \bar{I}_{7,2}(a_{13}) \right) \\ &\quad + 4\mathbf{w}_{14}^{(1)} \left( \bar{I}_2(a_{14}) + C_A \bar{I}_6(a_{14}) + C_A \bar{I}_{7,1}(a_{14}) + C_A \bar{I}_{7,2}(a_{14}) \right) \\ &\quad \left. + 2 \left( \mathbf{w}_{12}^{(3)} + \mathbf{w}_{34}^{(3)} \right) \bar{I}_3(a_{12}) + 4\mathbf{w}_{13}^{(3)} \left( \bar{I}_3(a_{13}) + \bar{I}_4(a_{13}) \right) + 4\mathbf{w}_{14}^{(3)} \left( \bar{I}_3(a_{14}) + \bar{I}_4(a_{14}) \right) \right] \end{aligned} \quad (20)$$



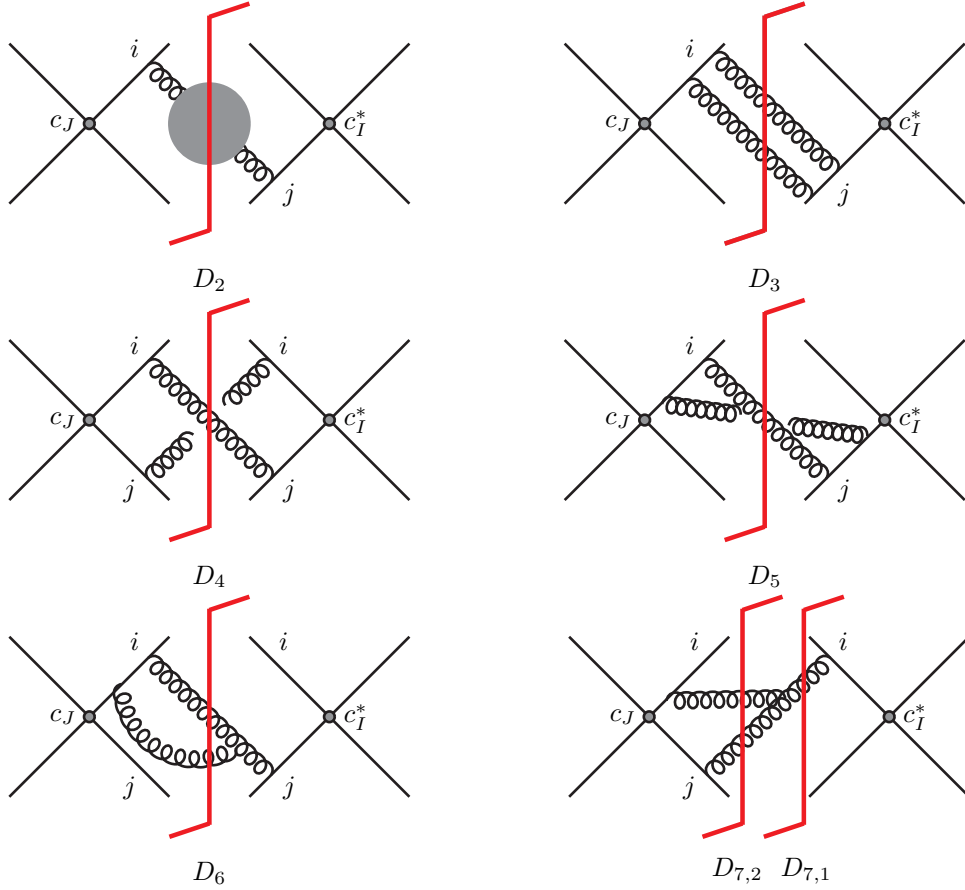


Figure 2: Two-Wilson-line integrals required in the calculation of the NNLO soft matrix.

$$\begin{aligned}
& + 4\mathbf{w}_{12}^{(9)} \bar{I}_4(a_{12}) + \left(\mathbf{w}_{12}^{(4)} + \mathbf{w}_{34}^{(4)}\right) \left(\bar{I}_4(a_{12}) + 2\bar{I}_5(a_{12})\right) \\
& + 2\mathbf{w}_{13}^{(4)} \left(\bar{I}_4(a_{13}) + 2\bar{I}_5(a_{13})\right) + 2\mathbf{w}_{14}^{(4)} \left(\bar{I}_4(a_{14}) + 2\bar{I}_5(a_{14})\right) \\
& + 4 \left(\mathbf{w}_{123}^{(8)} + \mathbf{w}_{314}^{(8)}\right) \bar{I}_8(a_{12}, a_{13}) + 4 \left(\mathbf{w}_{124}^{(8)} + \mathbf{w}_{324}^{(8)}\right) \bar{I}_8(a_{12}, a_{14}) + 8\mathbf{w}_{134}^{(8)} \bar{I}_8(a_{13}, a_{14}).
\end{aligned} \tag{21}$$

Three types of basic diagrams contribute to this sum, depending on whether the gluons attach to two, three, or four distinct Wilson lines. We organize this section by discussing each type of diagram in term, and give explicit results for the color factors and integrals appearing in (21). The results for the three and four parton diagrams turn out to be surprisingly simple, because the non-abelian exponentiation theorem constrains the coefficients of the color structures  $\mathbf{w}_{ijk}^{(8)}$  and  $\mathbf{w}_{ijkl}^{(9)}$  in (20). We discuss this further in Appendix B.

### 3.1 Two-Wilson-line integrals

The subset of non-vanishing two-Wilson-line integrals is familiar from other calculations of soft functions to NNLO [19, 24, 26]. The relevant Feynman diagrams are shown in Figure 2. Con-

verting these diagrams into integral expressions is straightforward, and leads to the following set:

$$\begin{aligned}
I_2(\omega, a_{ij}) &= -\pi^{1-\epsilon} (C_A(5-3\epsilon) - 2N_l(1-\epsilon)) \frac{\Gamma(2-\epsilon)}{\Gamma(4-2\epsilon)} \int [dk] \frac{n_i \cdot n_j \delta(\omega - n_0 \cdot k)}{n_i \cdot k n_j \cdot k (k^2)^{1+\epsilon}}, \\
I_3(\omega, a_{ij}) &= \int [dk] [dl] \frac{(n_i \cdot n_j)^2 \delta(\omega - n_0 \cdot (k+l))}{n_i \cdot k n_j \cdot (k+l) n_j \cdot l n_j \cdot (k+l)}, \\
I_4(\omega, a_{ij}) &= \int [dk] [dl] \frac{(n_i \cdot n_j)^2 \delta(\omega - n_0 \cdot (k+l))}{n_i \cdot k n_i \cdot l n_j \cdot k n_j \cdot l}, \\
I_5(\omega, a_{ij}) &= \int [dk] [dl] \frac{(n_i \cdot n_j)^2 \delta(\omega - n_0 \cdot (k+l))}{n_i \cdot k n_i \cdot (k+l) n_j \cdot k n_j \cdot (k+l)}, \\
I_6(\omega, a_{ij}) &= \int [dk] [dl] \frac{n_i \cdot n_j n_i \cdot (l-k) \delta(\omega - n_0 \cdot (k+l))}{n_i \cdot k n_i \cdot (k+l) n_j \cdot (k+l) (k+l)^2}, \\
I_{7,1}(\omega, a_{ij}) &= -\pi^{1-\epsilon} \Re[e^{-i\pi\epsilon}] \frac{\Gamma^2(1+\epsilon) \Gamma^3(-\epsilon)}{\Gamma(-2\epsilon)} \int [dq] \left( \frac{n_i \cdot n_j}{2n_i \cdot q n_j \cdot q} \right)^{1+\epsilon} \delta(\omega - n_0 \cdot q), \\
I_{7,2}(\omega, a_{ij}) &= \int [dk] [dl] \frac{n_i \cdot n_j n_j \cdot (k+2l) \delta(\omega - n_0 \cdot (k+l))}{n_i \cdot k n_j \cdot (k+l) n_j \cdot l (k+l)^2}. \tag{22}
\end{aligned}$$

The prefactors in  $I_2$  and  $I_{7,1}$  arise from the internal loop integrals, see for instance the discussion in [19, 26]. To evaluate the phase-space integrals we use light-cone coordinate techniques and parameterizations described in the Appendix of [26]. It is then relatively straightforward to derive results for the integrals in terms of hypergeometric functions, with the exception of  $I_5$  and  $I_{7,2}$ , which we evaluate as an expansion in  $\epsilon$ . In Appendix A we derive the results for the integral  $I_5$  as an example of the calculational procedure. Defining stripped integrals according to (with  $n > 1$ )

$$I_n(\omega, a_{ij}) = \pi^{2-2\epsilon} e^{-2\epsilon\gamma_E} \omega^{-1-4\epsilon} \bar{I}_n(a_{ij}) \tag{23}$$

the explicit results can be summarized as

$$\bar{I}_4(a) = \frac{8e^{2\epsilon\gamma_E} \Gamma^2(-\epsilon) \Gamma(-2\epsilon)}{\Gamma(1-2\epsilon) \Gamma(1-4\epsilon)} (1-a)^{-2\epsilon} [{}_2F_1(-\epsilon, -\epsilon, 1-\epsilon, a)]^2, \tag{24}$$

$$\begin{aligned}
\bar{I}_5(a) &= (1-a)^{-2\epsilon} \left[ -\frac{1}{\epsilon^3} + \frac{1}{\epsilon} \left( \frac{7\pi^2}{6} - 4H_2(a) \right) + \frac{62}{3}\zeta_3 - 12H_3(a) + 4H_{2,1}(a) \right. \\
&\quad \left. + \epsilon \left( \frac{\pi^4}{40} + \frac{14\pi^2}{3} H_2(a) - 36H_4(a) - 4H_{2,2}(a) + 12H_{3,1}(a) - 4H_{2,1,1}(a) \right) + \dots \right], \tag{25}
\end{aligned}$$

$$\bar{I}_3(a) = \frac{\bar{I}_4(a)}{2} - \bar{I}_5(a), \tag{26}$$

$$\bar{I}_6(a) = \frac{e^{2\epsilon\gamma_E} \Gamma^2(-\epsilon) \Gamma(-2\epsilon)}{\Gamma(2-2\epsilon) \Gamma(1-4\epsilon)} (1-a)^{-2\epsilon} {}_2F_1(-2\epsilon, -2\epsilon, 1-2\epsilon, a), \quad (27)$$

$$\bar{I}_2(a) = -(C_A(5-3\epsilon) - 2N_l(1-\epsilon)) \frac{2\Gamma(2-\epsilon)\Gamma(2-2\epsilon)}{\Gamma(4-2\epsilon)\Gamma(-\epsilon)} \bar{I}_6(a), \quad (28)$$

$$\bar{I}_{7,1}(a) = -\frac{2e^{2\epsilon\gamma_E} \Re[e^{-i\pi\epsilon}] \Gamma(-2\epsilon) \Gamma^2(-\epsilon) \Gamma^2(1+\epsilon)}{\Gamma(1-4\epsilon)} (1-a)^{-2\epsilon} {}_2F_1(-2\epsilon, -2\epsilon, 1-\epsilon, a), \quad (29)$$

$$\begin{aligned} \bar{I}_{7,2}(a) = (1-a)^{-2\epsilon} & \left[ -\frac{2}{\epsilon^3} + \frac{1}{\epsilon} \left( \frac{5\pi^2}{2} - 6H_2(a) \right) + \frac{139}{3} \zeta_3 - 8H_3(a) + 12H_{2,1}(a) \right. \\ & \left. + \epsilon \left( \frac{\pi^4}{36} + \frac{23\pi^2}{3} H_2(a) - 12H_4(a) - 4H_{2,2}(a) + 16H_{3,1}(a) - 24H_{2,1,1}(a) \right) + \dots \right]. \end{aligned} \quad (30)$$

To expand these in  $\epsilon$  we use (15) along with

$$\begin{aligned} {}_2F_1(-2\epsilon, -2\epsilon, 1-\epsilon, a) &= 1 + 4H_2(a)\epsilon^2 + (4H_3(a) - 12H_{2,1}(a))\epsilon^3 \\ &+ (4H_4(a) + 4H_{2,2}(a) - 12H_{3,1}(a) + 36H_{2,1,1}(a))\epsilon^4 + \dots \end{aligned} \quad (31)$$

These results can be related to those for a position-space soft function calculated in [24], and we have found full agreement with that work. They furthermore agree with results from [19] for  $a=0$  and from [26] for  $a=1$  as two special cases.

We must also evaluate the color factors. For these we find

$$\begin{aligned} \mathbf{w}_{ij}^{(2)} &= \mathbf{w}_{ij}^{(1)}, \\ \mathbf{w}_{ij}^{(3)} &= \frac{1}{d_R} \mathbf{T}_i^a \mathbf{T}_i^b \mathbf{T}_j^a \mathbf{T}_j^b, \\ \mathbf{w}_{ij}^{(4)} = \mathbf{w}_{ij}^{(5)} &= \frac{1}{d_R} \mathbf{T}_i^a \mathbf{T}_i^b \mathbf{T}_j^b \mathbf{T}_j^a = \mathbf{w}_{ij}^{(3)} - \frac{C_A}{2} \mathbf{w}_{ij}^{(1)}, \\ \mathbf{w}_{ij}^{(6)} = \mathbf{w}_{ij}^{(7,2)} = \mathbf{w}_{ij}^{(7,1)} &= \frac{1}{d_R} i f^{abc} \mathbf{T}_i^a \mathbf{T}_i^b \mathbf{T}_j^c = \frac{C_A}{2} \mathbf{w}_{ij}^{(1)}. \end{aligned} \quad (32)$$

The relation between  $\mathbf{w}_{ij}^{(3)}$  and  $\mathbf{w}_{ij}^{(4)}$ , along with the result that  $I_3 = I_4/2 - I_5$ , ensures that the bare function satisfies the non-abelian exponentiation theorem. We discuss this further in Appendix B. Results for the NLO matrices  $\mathbf{w}_{ij}^{(1)}$  were given in (18) and (19). In the  $q\bar{q}$  annihilation channel the remaining matrices evaluate to

$$\begin{aligned} \mathbf{w}_{12}^{(3)} = \mathbf{w}_{34}^{(3)} &= \frac{C_F}{2} \begin{pmatrix} N^2 - 1 & 0 \\ 0 & \frac{1}{4N^2} \end{pmatrix}, \\ \mathbf{w}_{13}^{(3)} = \mathbf{w}_{24}^{(3)} &= \frac{C_F}{2} \begin{pmatrix} 1 & \frac{N^2 - 2}{2N} \\ \frac{N^2 - 2}{2N} & \frac{N^4 - 3N^2 + 3}{4N^2} \end{pmatrix}, \end{aligned}$$

$$\mathbf{w}_{14}^{(3)} = \mathbf{w}_{23}^{(3)} = \frac{C_F}{2} \begin{pmatrix} 1 & -\frac{1}{N} \\ -\frac{1}{N} & \frac{N^2+3}{4N^2} \end{pmatrix}, \quad (33)$$

whereas in the gluon fusion channel they are

$$\begin{aligned} \mathbf{w}_{12}^{(3)} &= \frac{C_A}{2} \begin{pmatrix} 2N^2 & 0 & 0 \\ 0 & \frac{N^2}{4} & 0 \\ 0 & 0 & \frac{N^2-4}{4} \end{pmatrix}, \\ \mathbf{w}_{34}^{(3)} &= \frac{C_A}{2} \begin{pmatrix} \frac{(N^2-1)^2}{2N^2} & 0 & 0 \\ 0 & \frac{1}{4N^2} & 0 \\ 0 & 0 & \frac{N^2-4}{4N^4} \end{pmatrix}, \\ \mathbf{w}_{13}^{(3)} = \mathbf{w}_{24}^{(3)} &= \frac{C_A}{2} \begin{pmatrix} 1 & \frac{N}{4} & \frac{N^2-4}{4N} \\ \frac{N}{4} & \frac{N^2+2}{8} & \frac{N^2-4}{8} \\ \frac{N^2-4}{4N} & \frac{N^2-4}{8} & \frac{(N^2-2)(N^2-4)}{8N^2} \end{pmatrix}, \\ \mathbf{w}_{14}^{(3)} = \mathbf{w}_{23}^{(3)} &= \frac{C_A}{2} \begin{pmatrix} 1 & -\frac{N}{4} & \frac{N^2-4}{4N} \\ -\frac{N}{4} & \frac{N^2+2}{8} & -\frac{N^2-4}{8} \\ \frac{N^2-4}{4N} & -\frac{N^2-4}{8} & \frac{(N^2-2)(N^2-4)}{8N^2} \end{pmatrix}. \end{aligned} \quad (34)$$

### 3.2 Three-Wilson-line integrals

The three-Wilson-line integrals are of two basic types: the abelian graphs shown in Figure 3 and Figure 4, and the non-abelian graphs involving a three-gluon vertex shown in Figure 5.

We first discuss the abelian graphs. The two diagrams  $D_8^{(a)}$  and  $D_8^{(b)}$  in the first row of Figure 3 are obviously a convolution product of two NLO functions and introduce no further computational complications. The sum of these two diagrams gives a symmetric color structure

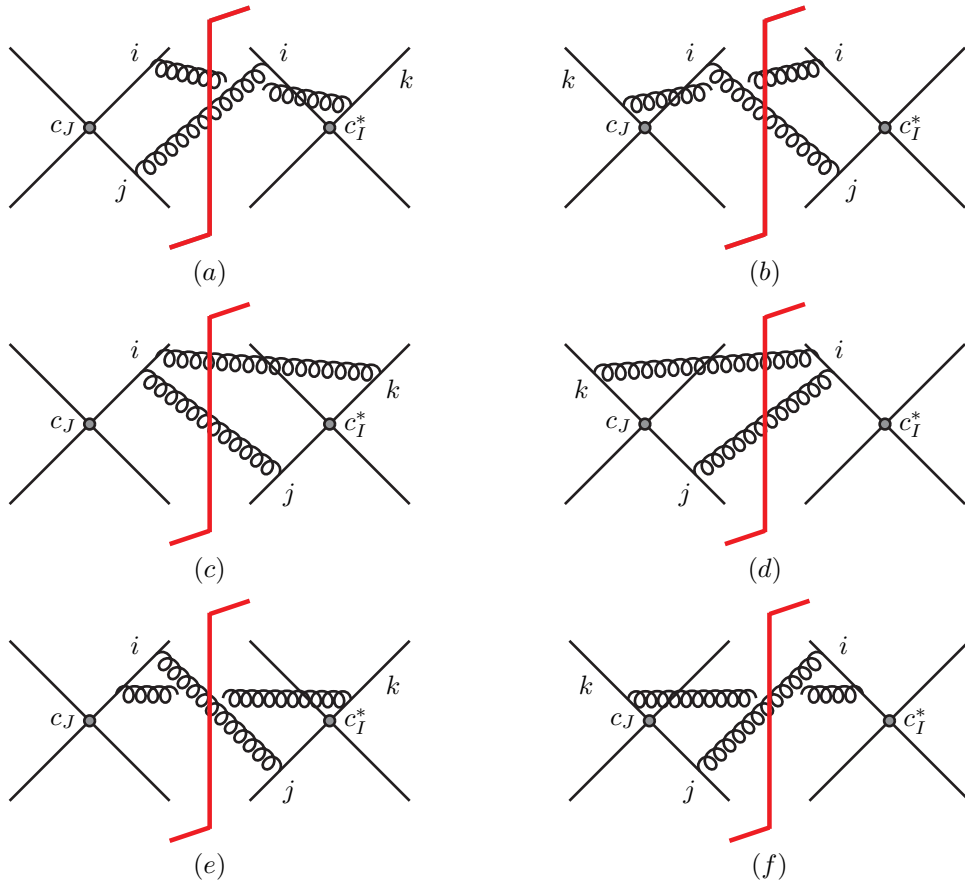
$$\mathbf{w}_{ijk}^{(8)} = \frac{1}{d_R} \{ \mathbf{T}_i^a, \mathbf{T}_i^b \} \mathbf{T}_j^a \mathbf{T}_k^b, \quad (35)$$

and the integral is

$$I_8(\omega, a_{ij}, a_{ik}) = \int [dk] [dl] \frac{n_i \cdot n_j \, n_i \cdot n_k \, \delta(\omega - n_0 \cdot (k+l))}{n_i \cdot k \, n_i \cdot l \, n_j \cdot k \, n_k \cdot l} = \pi^{2-2\epsilon} e^{-2\epsilon\gamma_E} \omega^{-1-4\epsilon} \bar{I}_8(a_{ij}, a_{ik}), \quad (36)$$

with

$$\begin{aligned} \bar{I}_8(a, a') &= \frac{8e^{2\epsilon\gamma_E} \Gamma^2(-\epsilon) \Gamma(-2\epsilon)}{\Gamma(1-2\epsilon) \Gamma(1-4\epsilon)} (1-a)^{-\epsilon} (1-a')^{-\epsilon} \\ &\quad \times {}_2F_1(-\epsilon, -\epsilon, 1-\epsilon, a) {}_2F_1(-\epsilon, -\epsilon, 1-\epsilon, a'). \end{aligned} \quad (37)$$



$D_8$

Figure 3: The abelian three-Wilson-line integrals required in the calculation of the NNLO soft matrix.

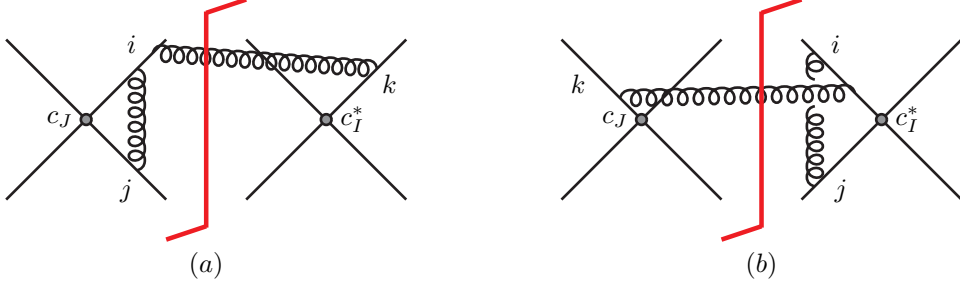


Figure 4: Example of a pair of mixed virtual-real one-particle cuts which adds up to a scaleless integral.

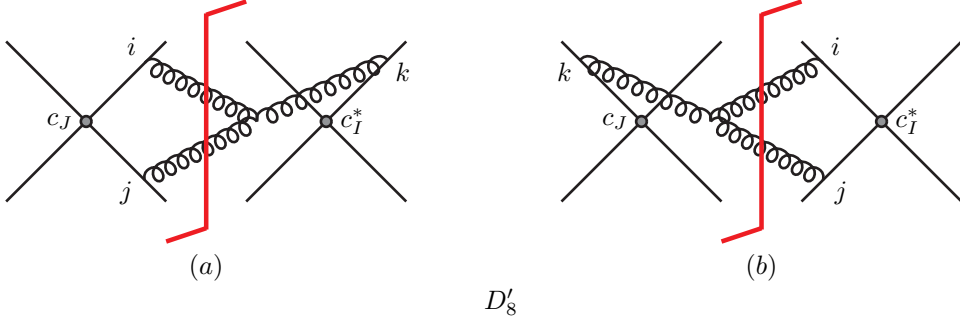


Figure 5: Examples of non-abelian three-Wilson-line integrals required in the calculation of the NNLO soft matrix.

Each of the four diagrams in the last two rows of Figure 3, on the other hand, are complicated functions of two distinct scalar products. However, the sums of the pairs (c) + (d) and (e) + (f) are proportional to symmetric color structure  $\mathbf{w}^{(8)}$ :

$$\begin{aligned}
 D_8^{(c)+(d)} &\rightarrow (\mathbf{T}_i^b \mathbf{T}_i^a + \mathbf{T}_i^a \mathbf{T}_i^b) \mathbf{T}_j^a \mathbf{T}_k^b \int [dk] [dl] \frac{n_i \cdot n_j n_i \cdot n_k \delta(\omega - n_0 \cdot (k+l))}{n_i \cdot l n_i \cdot (k+l) n_j \cdot k n_k \cdot l}, \\
 D_8^{(e)+(f)} &\rightarrow (\mathbf{T}_i^a \mathbf{T}_i^b + \mathbf{T}_i^b \mathbf{T}_i^a) \mathbf{T}_j^a \mathbf{T}_k^b \int [dk] [dl] \frac{n_i \cdot n_j n_i \cdot n_k \delta(\omega - n_0 \cdot (k+l))}{n_i \cdot k n_i \cdot (k+l) n_j \cdot k n_k \cdot l}. \quad (38)
 \end{aligned}$$

Furthermore, after partial fractioning, the sum of the two integrals yields the factorized integral (36). Therefore, these abelian diagrams do not introduce any new calculational complications. In Appendix B we explain how the non-abelian exponentiation theorem implies the simple factorized form of the integral multiplying the symmetric color structure (35). The color matrices for the  $q\bar{q}$  channel are

$$\begin{aligned}
 \mathbf{w}_{123}^{(8)} = \mathbf{w}_{214}^{(8)} = \mathbf{w}_{314}^{(8)} = \mathbf{w}_{423}^{(8)} &= \frac{C_F}{2} \begin{pmatrix} 0 & \frac{N^2-2}{2N} \\ \frac{N^2-2}{2N} & -\frac{N^2-2}{2N^2} \end{pmatrix}, \\
 \mathbf{w}_{124}^{(8)} = \mathbf{w}_{213}^{(8)} = \mathbf{w}_{324}^{(8)} = \mathbf{w}_{413}^{(8)} &= \frac{C_F}{2} \begin{pmatrix} 0 & -\frac{N^2-2}{2N} \\ -\frac{N^2-2}{2N} & -\frac{1}{N^2} \end{pmatrix},
 \end{aligned}$$

$$\mathbf{w}_{134}^{(8)} = \mathbf{w}_{234}^{(8)} = \mathbf{w}_{312}^{(8)} = \mathbf{w}_{412}^{(8)} = \frac{C_F}{2} \begin{pmatrix} -2 & -\frac{N^2-4}{2N} \\ -\frac{N^2-4}{2N} & \frac{N^2-3}{2N^2} \end{pmatrix}, \quad (39)$$

while those for the  $gg$  channel are

$$\begin{aligned} \mathbf{w}_{123}^{(8)} = \mathbf{w}_{214}^{(8)} &= \frac{C_A}{2} \begin{pmatrix} 0 & \frac{3}{2}N & 0 \\ \frac{3}{2}N & \frac{N^2}{4} & \frac{N^2-4}{4} \\ 0 & \frac{N^2-4}{4} & \frac{N^2-4}{4} \end{pmatrix}, \\ \mathbf{w}_{124}^{(8)} = \mathbf{w}_{213}^{(8)} &= \frac{C_A}{2} \begin{pmatrix} 0 & -\frac{3}{2}N & 0 \\ -\frac{3}{2}N & \frac{N^2}{4} & -\frac{N^2-4}{4} \\ 0 & -\frac{N^2-4}{4} & \frac{N^2-4}{4} \end{pmatrix}, \\ \mathbf{w}_{134}^{(8)} = \mathbf{w}_{234}^{(8)} = \mathbf{w}_{312}^{(8)} = \mathbf{w}_{412}^{(8)} &= \frac{C_A}{2} \begin{pmatrix} -2 & 0 & -\frac{N^2-4}{2N} \\ 0 & -\frac{1}{2} & 0 \\ -\frac{N^2-4}{2N} & 0 & \frac{N^2-4}{2N^2} \end{pmatrix}, \\ \mathbf{w}_{314}^{(8)} = \mathbf{w}_{423}^{(8)} &= \frac{C_A}{2} \begin{pmatrix} 0 & \frac{N^2-2}{2N} & 0 \\ \frac{N^2-2}{2N} & -\frac{1}{4} & -\frac{N^2-4}{4N^2} \\ 0 & -\frac{N^2-4}{4N^2} & -\frac{N^2-4}{4N^2} \end{pmatrix}, \\ \mathbf{w}_{324}^{(8)} = \mathbf{w}_{413}^{(8)} &= \frac{C_A}{2} \begin{pmatrix} 0 & -\frac{N^2-2}{2N} & 0 \\ -\frac{N^2-2}{2N} & -\frac{1}{4} & \frac{N^2-4}{4N^2} \\ 0 & \frac{N^2-4}{4N^2} & -\frac{N^2-4}{4N^2} \end{pmatrix}. \end{aligned} \quad (40)$$

We now discuss one-particle cuts of three-Wilson-line abelian diagrams. These are first of all due to contributions of the type shown in the first row of Figure 3, but where the connection to parton  $k$  is moved to the other side of the cut. These diagrams factorize in an obvious way into a product of an NLO-type integral with a scaleless virtual correction and thus evaluate to zero. The one-particle cuts corresponding to the diagrams in the last two rows of that figure are more complicated. However, one can show that the sum of pairs of the type shown in Figure 4 reduces to the same scaleless integral mentioned above. Therefore, these one-particle cuts do not contribute to the soft function.

In addition to the abelian diagrams, we must also evaluate non-abelian ones of the type shown in Figure 5. However, the sum of diagrams in the figure vanishes due to its color structure. Written explicitly, the two diagrams give

$$D_8^{\prime(a)} \rightarrow i f^{abc} \mathbf{T}_i^a \mathbf{T}_j^b \mathbf{T}_k^c I_8', \quad (41)$$

$$D_8^{\prime(b)} \rightarrow -i f^{abc} \mathbf{T}_i^a \mathbf{T}_j^b \mathbf{T}_k^c I_8', \quad (42)$$

where

$$I_8' = \int [dk][dl] \frac{n_i^\mu n_j^\nu n_k^\rho [(2k+l)_\nu g_{\mu\rho} - (k+2l)_\mu g_{\rho\nu} + (l-k)_\rho g_{\nu\mu}]}{n_i \cdot k \, n_j \cdot l \, n_k \cdot (k+l) \, (k+l)^2}. \quad (43)$$

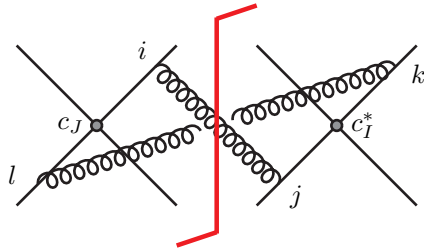


Figure 6: Four-Wilson-line diagrams contributing to the NNLO soft function.

The relative minus sign between the two diagrams originates from the fact that the gluon propagator carrying momentum  $k+l$  appears on opposite sides of the cut in the two diagrams<sup>4</sup>. Therefore, the sum of the two diagrams cancels. This is due to the structure of the color factors and not the integral itself, and is also true of one-particle cuts not shown in the figure. Interestingly enough, it would also be true if the velocity vectors were time-like, even though such anti-symmetric three-particle correlations are present in the anomalous dimension for massive particles [40, 41]. This is not a contradiction, since the soft function for massive heavy-quark production obeys an RG equation analogous to (49) below and the contribution of the three-particle correlations cancels between the sum of terms involving  $\gamma_s$  and  $\gamma_s^\dagger$ .

### 3.3 Four-Wilson-line integrals

We finally turn to the four-Wilson-line integrals. The two-particle cuts shown in Figure 6 are a convolution of NLO integrals and of the same form as  $I_4$  and  $I_8$ . The general integral reads

$$I_9(\omega, a_{ij}, a_{kl}) = \int [dk] [dl] \frac{n_i \cdot n_j n_k \cdot n_l \delta(\omega - n_0 \cdot (k+l))}{n_i \cdot k n_j \cdot k n_k \cdot l n_l \cdot l}, \quad (44)$$

and the color factor is

$$\mathbf{w}_{ij}^{(9)} = \frac{1}{d_R} \mathbf{T}_i^a \mathbf{T}_j^a \mathbf{T}_k^b \mathbf{T}_l^b \quad (i \neq j \neq k \neq l). \quad (45)$$

For two-to-two scattering considered here the relations between the different scalar products implies that we need only  $I_9(\omega, a_{ij}, a_{ij}) = I_4(\omega, a_{ij})$ , which we already took into account in writing (20). The explicit results for the color matrices are  $\mathbf{w}_{ij}^{(9)} = \mathbf{w}_{ij}^{(3)}$  in the  $q\bar{q}$  channel, and for the  $gg$  they read

$$\mathbf{w}_{12}^{(9)} = \frac{C_A}{2} \begin{pmatrix} N^2 - 1 & 0 & 0 \\ 0 & -\frac{1}{4} & 0 \\ 0 & 0 & -\frac{N^2 - 4}{4N^2} \end{pmatrix}, \quad (46)$$

<sup>4</sup>This change of sign also occurs in the diagrams generated from the non-abelian two Wilson-line diagrams  $D_6$  and  $D_{7,2}$  in Figure 2 by moving the two-gluon attachment to the other side of the cut. However, in those cases the order of the two color generators  $\mathbf{T}_i^a$  and  $\mathbf{T}_i^b$  is also exchanged, which compensates the sign change of the propagators.



and  $\mathbf{w}_{ij}^{(9)} = \mathbf{w}_{ij}^{(3)}$  for  $ij = 13, 14$ .

Also in this case there are one-particle cuts, but these always involve a scaleless loop graph and vanish.

## 4 Renormalization

The renormalized soft function is obtained from the bare one by multiplying on both sides by a matrix-valued UV renormalization factor. The structure of this renormalization factor follows from the RG equation for the soft function, which is simplest to discuss at the level of the Laplace-transformed function. We define this as

$$\tilde{\mathbf{s}}(L, t_1/M^2, \mu) = \int_0^\infty d\omega \exp\left(-\frac{\omega}{e^{\gamma_E} \mu e^{L/2}}\right) \mathbf{S}(\omega, t_1/M^2, \mu), \quad (47)$$

The integral transform is easily carried out from the bare function using

$$\int_0^\infty d\omega \exp[-b\omega] \omega^{-1-n\epsilon} = \Gamma(-n\epsilon) b^{\epsilon n}. \quad (48)$$

The RG equation for the Laplace-transformed function was derived in [12], using RG invariance of the cross section and the results for the hard, fragmentation, and parton luminosities. It reads

$$\begin{aligned} \frac{d}{d \ln \mu} \tilde{\mathbf{s}}\left(\ln \frac{M^2}{\mu^2}, t_1/M^2, \mu\right) = & \\ & - \left[ A(\alpha_s) \ln \frac{M^2}{\mu^2} + \gamma^{s\dagger}(t_1/M^2, \alpha_s) \right] \tilde{\mathbf{s}}\left(\ln \frac{M^2}{\mu^2}, t_1/M^2, \mu\right) \\ & - \tilde{\mathbf{s}}\left(\ln \frac{M^2}{\mu^2}, t_1/M^2, \mu\right) \left[ A(\alpha_s) \ln \frac{M^2}{\mu^2} + \gamma^s(t_1/M^2, \alpha_s) \right], \end{aligned} \quad (49)$$

where  $A = 2C_F \gamma_{\text{cusp}}$  in the  $q\bar{q}$  channel and  $A = (C_A + C_F) \gamma_{\text{cusp}}$  in the  $gg$  channel, and

$$\gamma^s(t_1/M^2, \alpha_s) = \gamma^h(t_1/M^2, \alpha_s) + [2\gamma^\phi(\alpha_s) + 2\gamma^{\phi_q}(\alpha_s)] \mathbf{1}. \quad (50)$$

The non-trivial matrix structure of the soft anomalous dimension is related to that in the hard function and is expressed through the function  $\gamma^h$ , which for the different channels is

$$\gamma_{q\bar{q}}^h = 4\gamma^q(\alpha_s) \mathbf{1} + N \gamma_{\text{cusp}}(\alpha_s) \left( \ln \frac{-t_1}{M^2} + i\pi \right) \begin{pmatrix} 0 & 0 \\ 0 & 1 \end{pmatrix} + \gamma_{\text{cusp}}(\alpha_s) \ln \frac{t_1^2}{u_1^2} \begin{pmatrix} 0 & \frac{C_F}{2N} \\ 1 & -\frac{1}{N} \end{pmatrix}, \quad (51)$$

and

$$\gamma_{gg}^h = [2\gamma^g(\alpha_s) + 2\gamma^q(\alpha_s)] \mathbf{1}$$

$$+ N\gamma_{\text{cusp}}(\alpha_s) \left( \ln \frac{-t_1}{M^2} + i\pi \right) \begin{pmatrix} 0 & 0 & 0 \\ 0 & 1 & 0 \\ 0 & 0 & 1 \end{pmatrix} + \gamma_{\text{cusp}}(\alpha_s) \ln \frac{t_1^2}{u_1^2} \begin{pmatrix} 0 & \frac{1}{2} & 0 \\ 1 & -\frac{N}{4} & \frac{N^2-4}{4N} \\ 0 & \frac{N}{4} & -\frac{N}{4} \end{pmatrix}. \quad (52)$$

Explicit results for the expansion coefficients defined as

$$A(\alpha_s) = \frac{\alpha_s}{4\pi} A_0 + \left( \frac{\alpha_s}{4\pi} \right)^2 A_1 + \dots, \quad (53)$$

and analogously for the other functions can be found in the the Appendix of [12].

Given the structure of the RG equations, we define the relationship between the bare and renormalized soft functions according to

$$\tilde{\mathbf{s}} = \mathbf{Z}_s^\dagger \tilde{\mathbf{s}}_{\text{bare}} \mathbf{Z}_s. \quad (54)$$

The bare soft function does not depend on  $\mu$ . This implies an RG equation for the renormalization factor which can be integrated to solve for its explicit expansion in  $\epsilon$  (see, e.g., [31]). This yields

$$\begin{aligned} \ln \mathbf{Z}_s &= \frac{\alpha_s}{4\pi} \left( -\frac{A_0}{2\epsilon^2} + \frac{A_0 L + \gamma_0^s}{2\epsilon} \right) \\ &+ \left( \frac{\alpha_s}{4\pi} \right)^2 \left[ \frac{3A_0\beta_0}{8\epsilon^3} + \frac{-A_1 - 2\beta_0(A_0 L + \gamma_0^s)}{8\epsilon^2} + \frac{A_1 L + \gamma_1^s}{4\epsilon} \right] + \dots. \end{aligned} \quad (55)$$

Defining expansion coefficients of the renormalization factor and Laplace-transformed functions in units of  $\alpha_s/4\pi$  as in (5), the renormalized NNLO function in Laplace space is given by

$$\begin{aligned} \tilde{\mathbf{s}}^{(2)}(L, t_1/M^2, \mu) &= \tilde{\mathbf{s}}_{\text{bare}}^{(2)} + \mathbf{Z}_s^{\dagger(2)} \tilde{\mathbf{s}}^{(0)} + \tilde{\mathbf{s}}^{(0)} \mathbf{Z}_s^{(2)} \\ &+ \mathbf{Z}_s^{\dagger(1)} \tilde{\mathbf{s}}_{\text{bare}}^{(1)} + \tilde{\mathbf{s}}_{\text{bare}}^{(1)} \mathbf{Z}_s^{(1)} + \mathbf{Z}_s^{\dagger(1)} \tilde{\mathbf{s}}^{(0)} \mathbf{Z}_s^{(1)} - \frac{\beta_0}{\epsilon} \tilde{\mathbf{s}}_{\text{bare}}^{(1)}. \end{aligned} \quad (56)$$

Evaluating this equation, we find that the renormalized function on the left-hand side is indeed finite in the limit  $\epsilon \rightarrow 0$ . This shows that the renormalization factor (55) following from the RG equation deduced from the factorization formula (1) is correct, or can otherwise be viewed as a cross-check on our calculations. The explicit expressions for the renormalized functions are rather lengthy and we relegate them to Appendix C. The terms proportional to powers of  $L$  in the renormalized function are in agreement with the approximate NNLO formulas mentioned in [12], while the  $L$ -independent pieces are new.

## 5 Conclusions

We evaluated the NNLO corrections to the soft function needed to describe the pair invariant mass distribution in top-quark pair production at hadron colliders in the small-mass limit. At the technical level, this required us to obtain real-emission type corrections related to a product of Wilson-loop operators depending on four light-like Wilson lines. This is the first NNLO calculation of a soft function which involves non-trivial matrix structure in color space. We showed that the IR structure of the bare function is consistent with known expressions for the two-loop anomalous dimension matrix derived in [12]. The final results, given in the Appendix, turned out to be rather simple. This is because in the sum of all diagrams contributions from integrals involving three or more Wilson lines multiply a color structure whose coefficient is constrained by the non-abelian exponentiation theorem to be a product of NLO integrals. The non-abelian three-parton graphs are not constrained by non-abelian exponentiation, but these vanish after summing over all diagrams.

Combined with known NNLO results for heavy-quark fragmentation functions and virtual corrections to two-to-two processes, our calculations will allow an evaluation of the invariant mass distribution in the small-mass limit at the level of a full virtual plus soft approximation. This will provide valuable information concerning the importance of higher-order corrections to NLO+NNLL predictions from [4]. Moreover, by an appropriate modification of the delta-function constraint in the definition (4), we can immediately obtain the soft function needed to study single-particle distributions in the  $p_T$  and rapidity of the top quark to the same level of accuracy, opening up the possibility of studying higher-order corrections to the results of [42, 43]. Finally, we anticipate applications for threshold resummation in dijet production.

## Acknowledgments

We would like to thank Matthias Neubert for useful discussions. This research was supported in part by the PSC-CUNY Award N. 64133-00 42, by the NSF grant PHY-1068317, by the German Research Foundation under grant NE398/3-1, 577401: *Applications of Effective Field Theories to Collider Physics*, by the European Commission through the *LHCPheNet* Initial Training Network PITN-GA-2010-264564, and by the Schweizer Nationalfonds under grant 200020-141360/1.

## A Calculation of $I_5$ as an example

Written out explicitly, the integral  $I_5$  reads (with  $\delta^+(k^2) = \delta(k^2)\theta(k^0)$ )

$$\begin{aligned} I_5(\omega, a_{ij}) &= \int d^d l_1 d^d l_2 \frac{(n_i \cdot n_j)^2 \delta^+(l_1^2) \delta^+(l_2^2) \delta(\omega - n_0 \cdot (l_1 + l_2))}{n_i \cdot l_1 n_i \cdot (l_1 + l_2) n_j \cdot l_1 n_j \cdot (l_1 + l_2)} \\ &= \int d^d k \frac{n_i \cdot n_j \delta(\omega - n_0 \cdot k)}{n_i \cdot k n_j \cdot k} \int d^d l_1 d^d l_2 \frac{n_i \cdot n_j \delta^+(l_1^2) \delta^+(l_2^2) \delta^{(d)}(k - l_1 - l_2)}{n_i \cdot l_1 n_j \cdot l_1} \end{aligned}$$

$$\begin{aligned}
&= \int d^d k \frac{n_i \cdot n_j \delta(\omega - n_0 \cdot k)}{n_i \cdot k n_j \cdot k} 2\pi^{1-\epsilon} \frac{\Gamma(-\epsilon)}{\Gamma(1-2\epsilon)} \left( \frac{2 n_i \cdot k n_j \cdot k}{n_i \cdot n_j} \right)^\epsilon \\
&\quad \times (k^2)^{-1-2\epsilon} {}_2F_1 \left( -\epsilon, -\epsilon, 1-\epsilon, \frac{n_i \cdot n_j k_T^2}{2 n_i \cdot k n_j \cdot k} \right). \tag{57}
\end{aligned}$$

To derive the equality in the third line we used the auxiliary integral given in [24, 26]. The remaining  $d$ -dimensional integral over  $k$  can be solved using the steps outlined in [26]. We first define light-cone coordinates

$$\begin{aligned}
k^\mu &= k_+ \frac{n_i^\mu}{\sqrt{2 n_i \cdot n_j}} + k_- \frac{n_j^\mu}{\sqrt{2 n_i \cdot n_j}} + k_\perp^\mu, \\
k_+ &= \frac{n_j \cdot k}{\sqrt{n_i \cdot n_j/2}}, \quad k_- = \frac{n_i \cdot k}{\sqrt{n_i \cdot n_j/2}}, \quad k_T^2 = -k_\perp^2,
\end{aligned}$$

and use these to parameterize the integral over  $k$ . This yields

$$\begin{aligned}
I_5(\omega, a_{ij}) &= \frac{2^{2-2\epsilon} \pi^{1-2\epsilon} \Gamma(-\epsilon) \Gamma(1-\epsilon)}{\Gamma^2(1-2\epsilon)} \int dk_+ dk_- \int_0^\infty dk_T k_T^{1-2\epsilon} \int_{-1}^1 d \cos \theta \sin^{-1-2\epsilon} \theta \\
&\quad \times (k_+ k_-)^{-1+\epsilon} (k_+ k_- - k_T^2)^{-1-2\epsilon} {}_2F_1 \left( -\epsilon, -\epsilon, 1-\epsilon, \frac{k_T^2}{k_+ k_-} \right) \\
&\quad \times \delta \left( \omega - \frac{k_+ n_{0-} + k_- n_{0+}}{2} + n_{0T} k_T \cos \theta \right). \tag{58}
\end{aligned}$$

We then make the change of variables

$$\begin{aligned}
k_+ &= \frac{\omega}{n_{0-}} x y, \quad k_- = \frac{\omega}{n_{0+}} (1-x) y, \quad dk_+ dk_- = \frac{\omega^2}{n_{0+} n_{0-}} y dx dy, \\
k_T &= \frac{\omega}{\sqrt{n_{0+} n_{0-}}} \sqrt{x(1-x)} y u, \quad dk_T = \frac{\omega}{\sqrt{n_{0+} n_{0-}}} \sqrt{x(1-x)} y du,
\end{aligned}$$

and express the light-cone components of  $n_0$  in terms of  $a_{ij}$  to arrive at

$$\begin{aligned}
I_5(\omega, a_{ij}) &= \frac{2^{2+2\epsilon} \pi^{1-2\epsilon} \Gamma(-\epsilon) \Gamma(1-\epsilon)}{\Gamma^2(1-2\epsilon)} \omega^{-1-4\epsilon} (1-a_{ij})^{-2\epsilon} \\
&\quad \times \int_0^1 dx \int_0^\infty dy \int_{-1}^1 d \cos \theta \sin^{-1-2\epsilon} \theta \int_0^1 du [x(1-x)]^{-1-2\epsilon} y^{-1-4\epsilon} u^{1-2\epsilon} (1-u^2)^{-1-2\epsilon} \\
&\quad \times {}_2F_1(-\epsilon, -\epsilon, 1-\epsilon, u^2) \delta \left( 1 - \frac{y}{2} + \sqrt{a_{ij} x(1-x)} y u \cos \theta \right). \tag{59}
\end{aligned}$$

We next perform the  $y$ -integration using the delta-function constraint and integrate over  $\cos \theta$ , generating a hypergeometric function written in the first equality below. After that we perform

a change of variables to the argument of this hypergeometric function, integrate, and perform another change of variables to the argument of the original hypergeometric function. Explicitly,

$$\begin{aligned}
I_5(\omega, a_{ij}) &= \frac{4 \pi^{2-2\epsilon} \Gamma(-\epsilon)}{\Gamma(1-\epsilon) \Gamma(1-2\epsilon)} \omega^{-1-4\epsilon} (1-a)^{-2\epsilon} \\
&\times \int_0^1 du u^{1-2\epsilon} (1-u^2)^{-1-2\epsilon} {}_2F_1(-\epsilon, -\epsilon, 1-\epsilon, u^2) \\
&\times \int_0^1 dx [x(1-x)]^{-1-2\epsilon} {}_2F_1\left(\frac{1}{2}-2\epsilon, -2\epsilon, 1-\epsilon, 4a_{ij}x(1-x)u^2\right) \\
&= \frac{2^{3+4\epsilon} \pi^{2-2\epsilon} \Gamma(-\epsilon)}{\Gamma(1-\epsilon) \Gamma(1-2\epsilon)} \omega^{-1-4\epsilon} (1-a_{ij})^{-2\epsilon} \\
&\times \int_0^1 du u^{1-2\epsilon} (1-u^2)^{-1-2\epsilon} {}_2F_1(-\epsilon, -\epsilon, 1-\epsilon, u^2) \\
&\times \int_0^1 dv v^{-1-2\epsilon} (1-v)^{-1/2} {}_2F_1\left(\frac{1}{2}-2\epsilon, -2\epsilon, 1-\epsilon, a_{ij}u^2v\right) \\
&= \frac{4 \pi^{2-2\epsilon} \Gamma(-\epsilon) \Gamma(-2\epsilon)}{\Gamma(1-\epsilon) \Gamma(1-4\epsilon)} \omega^{-1-4\epsilon} (1-a_{ij})^{-2\epsilon} \\
&\times \int_0^1 dt t^{-\epsilon} (1-t)^{-1-2\epsilon} {}_2F_1(-\epsilon, -\epsilon, 1-\epsilon, t) {}_2F_1(-2\epsilon, -2\epsilon, 1-\epsilon, a_{ij}t). \quad (60)
\end{aligned}$$

The integral over the hypergeometric functions is sufficiently complicated that we evaluate it as an expansion in  $\epsilon$ . This is achieved using the standard identity

$$(1-t)^{-1-n\epsilon} = -\frac{1}{n\epsilon} \delta(1-t) + \sum_{m=0}^{\infty} \frac{(-n\epsilon)^m}{m!} \left[ \frac{\ln^m(1-t)}{1-t} \right]_+, \quad (61)$$

and evaluating the integrals over the plus distributions after expanding the other parts of the integral in  $\epsilon$ . This leads to parametric integrals over HPLs. Some of these are straightforward, and even the most difficult ones are not hard to handle by deriving and solving differential equations with respect to the parameter  $a_{ij}$ , yielding the result given in Section 3.

## B Constraints from non-abelian exponentiation

In this section we briefly explain the consistency of our results with the non-abelian exponentiation theorem [27, 28]. In general, this theorem states that the soft function can be written as the exponential of a simpler quantity. In particular, in the language of [28], the exponent receives contributions only from diagrams involving single connected webs. For us, the important point is that this theorem implies that after summing over all diagrams the coefficients of

certain color factors in the NNLO function are determined by exponentiating the NLO result. This exponentiation occurs in position or Laplace space rather than momentum space. We find it convenient to work with the Laplace-space function (47). Our procedure is to take the exponential of the one-loop bare function and expand it to second order:

$$\frac{1}{d_R} \exp \left[ - \sum_{i,j} \mathbf{T}_i \cdot \mathbf{T}_j \tilde{I}_1(L, a_{ij}) \right] = \frac{1}{d_R} \left[ 1 - \sum_{i,j} \mathbf{T}_i \cdot \mathbf{T}_j \tilde{I}_1(L, a_{ij}) + \frac{1}{2} \sum_{i,j,k,l} \mathbf{T}_i \cdot \mathbf{T}_j \mathbf{T}_k \cdot \mathbf{T}_l \tilde{I}_1(L, a_{ij}) \tilde{I}_1(L, a_{kl}) + \dots \right]. \quad (62)$$

The term on the second line produces two, three and four parton terms whose structure must be reproduced in our explicit results. First, we can write the two parton terms as

$$\begin{aligned} & \frac{2}{d_R} \left( \mathbf{T}_1^a \cdot \mathbf{T}_2^a \mathbf{T}_1^b \cdot \mathbf{T}_2^b \tilde{I}_1^2(L, a_{12}) + \mathbf{T}_3^a \cdot \mathbf{T}_4^a \mathbf{T}_3^b \cdot \mathbf{T}_4^b \tilde{I}_1^2(L, a_{12}) \right. \\ & \left. + 2\mathbf{T}_1^a \cdot \mathbf{T}_3^a \mathbf{T}_1^b \cdot \mathbf{T}_3^b \tilde{I}_1^2(L, a_{13}) + 2\mathbf{T}_1^a \cdot \mathbf{T}_4^a \mathbf{T}_1^b \cdot \mathbf{T}_4^b \tilde{I}_1^2(L, a_{14}) \right). \end{aligned} \quad (63)$$

We thus expect the coefficient of  $\mathbf{w}_{ij}^{(3)}$  to be restricted by the non-abelian exponentiation theorem, and a relation between  $\tilde{I}_3, \tilde{I}_4, \tilde{I}_5$  and the NLO integral. Indeed, we have already made explicit in (22) that  $I_3 = I_4/2 - I_5$ , and one can easily verify that  $\tilde{I}_4 = \tilde{I}_1^2$ . After rewriting the color factor  $\mathbf{w}_{ij}^{(4)}$  as in the last equality in (32) and performing the sum over legs one can then show that the coefficient of  $\mathbf{w}_{ij}^{(3)}$  in (21) is proportional to the factorized integral  $\tilde{I}_4$ , as required. The remaining two-Wilson-line integrals are proportional to the NLO matrix  $\mathbf{w}_{ij}^{(1)}$  and are thus single connected webs which contribute to the second-order expansion of the exponent directly.

Next we deal with three-parton terms. To understand their structure we consider the concrete example where two gluons attach to the parton with velocity  $n_1$  and the other two to the partons with velocity  $n_2$  and  $n_3$ . The contribution of these terms to (62) is

$$\frac{2}{d_R} \left( \mathbf{T}_1^a \cdot \mathbf{T}_2^a \mathbf{T}_1^b \cdot \mathbf{T}_3^b + \mathbf{T}_1^a \cdot \mathbf{T}_3^a \mathbf{T}_1^b \cdot \mathbf{T}_2^b \right) \tilde{I}_1(L, a_{12}) \tilde{I}_1(L, a_{13}) = 2\mathbf{w}_{123}^{(8)} \tilde{I}_1(L, a_{12}) \tilde{I}_1(L, a_{13}), \quad (64)$$

where we have used that the color matrices for different partons commute. The above relation implies that  $\tilde{I}_1(L, a_{12}) \tilde{I}_1(L, a_{13}) = \tilde{I}_8(L, a_{12}, a_{13})$ , and one can confirm that this is indeed the case. Including all permutations in the expansion of the exponential, we reproduce the contributions proportional to the  $\mathbf{w}_{ijk}^{(8)}$  in (21).

Finally, we turn to the four-parton terms, considering as an example the case where the two partons with velocity  $n_1$  and  $n_2$  are connected to each other. These contribute to (62) as

$$\frac{4}{d_R} \mathbf{T}_1^a \cdot \mathbf{T}_2^a \mathbf{T}_3^b \cdot \mathbf{T}_4^b \tilde{I}_1(a_{12}) \tilde{I}_1(a_{34}) = 4\mathbf{w}_{12}^{(9)} \tilde{I}_4(a_{12}). \quad (65)$$

This accounts explicitly for the four-parton term  $\mathbf{w}_{12}^{(9)} I_4(a_{12})$  (21). The remaining four-parton terms appear as  $\mathbf{w}_{ij}^{(3)} I_4(a_{ij})$ .

## C Renormalized Soft Functions

We list here the results for the renormalized soft function in the  $q\bar{q}$  and  $gg$  production channels. For the sake of brevity we set  $N = 3$  and take into account that the soft function is symmetric. In the following, we indicate the element  $ij$  of the matrix  $\tilde{s}_k^{(n)}$  ( $k \in \{q\bar{q}, gg\}$ ) as  $\tilde{s}_{kij}^{(n)}$ .

### C.1 Quark Annihilation Channel

The elements of the NLO soft matrix in Laplace space are

$$\begin{aligned}
\tilde{s}_{qq11}^{(1)} &= 16L^2 + \frac{8}{3}\pi^2, \\
\tilde{s}_{qq12}^{(1)} &= \frac{8\pi^2}{9} + \frac{16}{3}LH_0(x_t) + \frac{16}{3}LH_1(x_t) - \frac{16}{3}H_2(x_t) + \frac{16}{3}H_{0,0}(x_t) + \frac{16}{3}H_{1,0}(x_t) - \frac{16}{3}H_{1,1}(x_t), \\
\tilde{s}_{qq22}^{(1)} &= \frac{32L^2}{9} + \frac{44\pi^2}{27} + \frac{56}{9}LH_0(x_t) - \frac{16}{9}LH_1(x_t) + \frac{16}{9}H_2(x_t) + \frac{56}{9}H_{0,0}(x_t) + \frac{56}{9}H_{1,0}(x_t) \\
&\quad + \frac{16}{9}H_{1,1}(x_t). \tag{66}
\end{aligned}$$

The elements of the NNLO soft matrix in Laplace space are

$$\begin{aligned}
\tilde{s}_{qq11}^{(2)} &= \frac{19424}{27} - \frac{6464}{9}L + \frac{1072}{3}L^2 - \frac{176}{3}L^3 + \frac{128}{3}L^4 - \frac{2624}{81}N_l + \frac{896}{27}LN_l - \frac{160}{9}L^2N_l \\
&\quad + \frac{32}{9}L^3N_l + \frac{268}{9}\pi^2 - \frac{16}{9}L^2\pi^2 - \frac{40}{27}N_l\pi^2 - \frac{56}{9}\pi^4 + \frac{64}{9}L\pi^2H_0(x_t) + \frac{64}{9}L\pi^2H_1(x_t) \\
&\quad + \left[ \frac{128}{3}L^2 - \frac{64}{9}\pi^2 \right] H_2(x_t) - \frac{128}{3}LH_3(x_t) - 128H_4(x_t) + \left[ \frac{128}{3}L^2 + \frac{64}{9}\pi^2 \right] H_{0,0}(x_t) \\
&\quad + \frac{128}{3}L^2H_{1,0}(x_t) + \frac{64}{9}\pi^2H_{1,0}(x_t) + \left[ \frac{128}{3}L^2 - \frac{64}{9}\pi^2 \right] H_{1,1}(x_t) - \frac{128}{3}LH_{1,2}(x_t) \\
&\quad - 128H_{1,3}(x_t) + \frac{128}{3}LH_{2,0}(x_t) - 128LH_{2,1}(x_t) - \frac{128}{3}H_{2,2}(x_t) - \frac{128}{3}H_{3,0}(x_t) \\
&\quad + \frac{128}{3}H_{3,1}(x_t) + 128LH_{0,0,0}(x_t) + 128LH_{1,0,0}(x_t) + \frac{128}{3}LH_{1,1,0}(x_t) \\
&\quad - 128LH_{1,1,1}(x_t) - \frac{128}{3}H_{1,1,2}(x_t) - \frac{128}{3}H_{1,2,0}(x_t) + \frac{128}{3}H_{1,2,1}(x_t) + \frac{128}{3}H_{2,0,0}(x_t) \\
&\quad - 128H_{2,1,0}(x_t) + 128H_{2,1,1}(x_t) + 128H_{0,0,0,0}(x_t) + 128H_{1,0,0,0}(x_t) + \frac{128}{3}H_{1,1,0,0}(x_t) \\
&\quad - 128H_{1,1,1,0}(x_t) + 128H_{1,1,1,1}(x_t) - \frac{176}{3}\zeta_3 + 672L\zeta_3 + \frac{32}{9}N_l\zeta_3,
\end{aligned}$$

$$\begin{aligned}
\tilde{s}_{qq^{12}}^{(2)} = & \frac{536}{27}\pi^2 - \frac{88}{9}L\pi^2 + \frac{128}{27}L^2\pi^2 - \frac{80}{81}N_l\pi^2 + \frac{16}{27}LN_l\pi^2 - \frac{124}{135}\pi^4 + \left[ -\frac{3232}{27} \right. \\
& + \frac{1072}{9}L - \frac{88}{3}L^2 + \frac{256}{9}L^3 + \frac{448}{81}N_l - \frac{160}{27}LN_l + \frac{16}{9}L^2N_l - \frac{88}{9}\pi^2 + \frac{208}{27}L\pi^2 \\
& \left. + \frac{16}{27}N_l\pi^2 + 112\zeta_3 \right] H_0(x_t) + \left[ -\frac{3232}{27} + \frac{1072}{9}L - \frac{88}{3}L^2 + \frac{256}{9}L^3 + \frac{448}{81}N_l - \frac{160}{27}LN_l \right. \\
& \left. + \frac{16}{9}L^2N_l - \frac{88}{9}\pi^2 + \frac{64}{27}L\pi^2 + \frac{16}{27}N_l\pi^2 + 144\zeta_3 \right] H_1(x_t) + \left[ -\frac{1072}{9} + \frac{176}{3}L \right. \\
& \left. - \frac{32}{3}L^2 + \frac{160}{27}N_l - \frac{32}{9}LN_l - \frac{64}{27}\pi^2 \right] H_2(x_t) + \left[ -\frac{176}{3} - \frac{160}{9}L + \frac{32}{9}N_l \right] H_3(x_t) \\
& - \frac{64}{3}H_4(x_t) + \left[ \frac{1072}{9} - \frac{176}{3}L + \frac{704}{9}L^2 - \frac{160}{27}N_l + \frac{32}{9}LN_l + \frac{208}{27}\pi^2 \right] H_{0,0}(x_t) \\
& + \left[ \frac{1072}{9} - \frac{176}{3}L + \frac{416}{9}L^2 - \frac{160}{27}N_l + \frac{32}{9}LN_l + \frac{64}{27}\pi^2 \right] H_{1,0}(x_t) + \left[ -\frac{1072}{9} \right. \\
& \left. + \frac{176}{3}L - \frac{128}{3}L^2 + \frac{160}{27}N_l - \frac{32}{9}LN_l - \frac{208}{27}\pi^2 \right] H_{1,1}(x_t) + \left[ -\frac{176}{3} + \frac{128}{9}L \right. \\
& \left. + \frac{32}{9}N_l \right] H_{1,2}(x_t) - \frac{160}{3}H_{1,3}(x_t) + \left[ -\frac{176}{3} + \frac{448}{9}L + \frac{32}{9}N_l \right] H_{2,0}(x_t) \\
& + \left[ -\frac{176}{3} + \frac{32}{3}L + \frac{32}{9}N_l \right] H_{2,1}(x_t) - \frac{160}{9}H_{2,2}(x_t) + \frac{128}{9}H_{3,0}(x_t) + \frac{160}{9}H_{3,1}(x_t) \\
& + \left[ -\frac{176}{3} + \frac{448}{3}L + \frac{32}{9}N_l \right] H_{0,0,0}(x_t) + \left[ -\frac{176}{3} + \frac{352}{3}L + \frac{32}{9}N_l \right] H_{1,0,0}(x_t) \\
& + \left[ -\frac{176}{3} + \frac{160}{9}L + \frac{32}{9}N_l \right] H_{1,1,0}(x_t) + \left[ -\frac{176}{3} + \frac{128}{3}L + \frac{32}{9}N_l \right] H_{1,1,1}(x_t) \\
& - \frac{448}{9}H_{1,1,2}(x_t) - \frac{160}{9}H_{1,2,0}(x_t) - \frac{416}{9}H_{1,2,1}(x_t) + \frac{736}{9}H_{2,0,0}(x_t) - \frac{160}{3}H_{2,1,0}(x_t) \\
& + \frac{64}{3}H_{2,1,1}(x_t) + \frac{448}{3}H_{0,0,0,0}(x_t) + \frac{256}{3}H_{1,0,0,0}(x_t) + \frac{160}{9}H_{1,1,0,0}(x_t)
\end{aligned}$$



$$\begin{aligned}
& -\frac{256}{3}H_{1,1,1,0}(x_t) - \frac{128}{3}H_{1,1,1,1}(x_t), \\
\tilde{s}_{qq}^{(2)} = & \frac{38848}{243} - \frac{12928}{81}L + \frac{2144}{27}L^2 - \frac{352}{27}L^3 + \frac{256}{27}L^4 - \frac{5248}{729}N_l + \frac{1792}{243}LN_l \\
& - \frac{320}{81}L^2N_l + \frac{64}{81}L^3N_l + \frac{268}{9}\pi^2 - \frac{308}{27}L\pi^2 + \frac{416}{81}L^2\pi^2 - \frac{40}{27}N_l\pi^2 + \frac{56}{81}LN_l\pi^2 \\
& - \frac{994}{405}\pi^4 + \left[ -\frac{11312}{81} + \frac{3752}{27}L - \frac{308}{9}L^2 + \frac{896}{27}L^3 + \frac{1568}{243}N_l - \frac{560}{81}LN_l + \frac{56}{27}L^2N_l \right. \\
& \left. - \frac{308}{27}\pi^2 + \frac{856}{81}L\pi^2 + \frac{56}{81}N_l\pi^2 + \frac{392}{3}\zeta_3 \right] H_0(x_t) + \left[ \frac{3232}{81} - \frac{1072}{27}L + \frac{88}{9}L^2 - \frac{256}{27}L^3 \right. \\
& \left. - \frac{448}{243}N_l + \frac{160}{81}LN_l - \frac{16}{27}L^2N_l - \frac{308}{27}\pi^2 - \frac{80}{81}L\pi^2 + \frac{56}{81}N_l\pi^2 \right] H_1(x_t) + \left[ \frac{1072}{27} \right. \\
& \left. - \frac{176}{9}L + \frac{64}{27}L^2 - \frac{160}{81}N_l + \frac{32}{27}LN_l + \frac{80}{81}\pi^2 \right] H_2(x_t) + \left[ \frac{176}{9} + \frac{64}{9}L - \frac{32}{27}N_l \right] H_3(x_t) \\
& + \frac{32}{3}H_4(x_t) + \left[ \frac{3752}{27} - \frac{616}{9}L + \frac{2720}{27}L^2 - \frac{560}{81}N_l + \frac{112}{27}LN_l + \frac{856}{81}\pi^2 \right] H_{0,0}(x_t) \\
& + \left[ \frac{3752}{27} - \frac{616}{9}L + \frac{704}{27}L^2 - \frac{560}{81}N_l + \frac{112}{27}LN_l + \frac{352}{81}\pi^2 \right] H_{1,0}(x_t) + \left[ \frac{1072}{27} - \frac{176}{9}L \right. \\
& \left. + \frac{640}{27}L^2 - \frac{160}{81}N_l + \frac{32}{27}LN_l - \frac{424}{81}\pi^2 \right] H_{1,1}(x_t) + \left[ \frac{176}{9} - \frac{128}{9}L - \frac{32}{27}N_l \right] H_{1,2}(x_t) \\
& + \frac{64}{3}H_{1,3}(x_t) + \left[ -\frac{616}{9} + \frac{608}{9}L + \frac{112}{27}N_l \right] H_{2,0}(x_t) + \left[ \frac{176}{9} - \frac{64}{3}L - \frac{32}{27}N_l \right] H_{2,1}(x_t) \\
& + \frac{160}{9}H_{2,2}(x_t) + \frac{736}{9}H_{3,0}(x_t) + \frac{128}{9}H_{3,1}(x_t) + \left[ -\frac{616}{9} + \frac{608}{3}L + \frac{112}{27}N_l \right] H_{0,0,0}(x_t) \\
& + \left[ -\frac{616}{9} + 128L + \frac{112}{27}N_l \right] H_{1,0,0}(x_t) + \left[ -\frac{616}{9} - \frac{64}{9}L + \frac{112}{27}N_l \right] H_{1,1,0}(x_t) \\
& + \left[ \frac{176}{9} - \frac{128}{3}L - \frac{32}{27}N_l \right] H_{1,1,1}(x_t) + \frac{256}{9}H_{1,1,2}(x_t) + \frac{400}{9}H_{1,2,0}(x_t) + \frac{320}{9}H_{1,2,1}(x_t)
\end{aligned}$$

$$\begin{aligned}
& + \frac{1280}{9}H_{2,0,0}(x_t) + \frac{64}{3}H_{2,1,0}(x_t) + \frac{64}{3}H_{2,1,1}(x_t) + \frac{608}{3}H_{0,0,0,0}(x_t) + 128H_{1,0,0,0}(x_t) \\
& + \frac{608}{9}H_{1,1,0,0}(x_t) - 16H_{1,1,1,0}(x_t) + \frac{128}{3}H_{1,1,1,1}(x_t) - \frac{352}{27}\zeta_3 + \frac{448}{3}L\zeta_3 + \frac{64}{81}N_l\zeta_3. \quad (67)
\end{aligned}$$

## C.2 Gluon Fusion Channel

The elements of the NLO soft matrix in Laplace space are

$$\begin{aligned}
\tilde{s}_{gg11}^{(1)} &= 26L^2 + \frac{13}{3}\pi^2, \\
\tilde{s}_{gg12}^{(1)} &= 2\pi^2 + 12LH_0(x_t) + 12LH_1(x_t) - 12H_2(x_t) + 12H_{0,0}(x_t) + 12H_{1,0}(x_t) - 12H_{1,1}(x_t), \\
\tilde{s}_{gg13}^{(1)} &= 0, \\
\tilde{s}_{gg22}^{(1)} &= 13L^2 + \frac{11}{3}\pi^2 + 9LH_0(x_t) - 9LH_1(x_t) + 9H_2(x_t) + 9H_{0,0}(x_t) + 9H_{1,0}(x_t) + 9H_{1,1}(x_t), \\
\tilde{s}_{gg23}^{(1)} &= \frac{5}{6}\pi^2 + 5LH_0(x_t) + 5LH_1(x_t) - 5H_2(x_t) + 5H_{0,0}(x_t) + 5H_{1,0}(x_t) - 5H_{1,1}(x_t), \\
\tilde{s}_{gg33}^{(1)} &= \frac{55}{27}\pi^2 + \frac{65L^2}{9} + 5LH_0(x_t) - 5LH_1(x_t) + 5H_2(x_t) + 5H_{0,0}(x_t) + 5H_{1,0}(x_t) + 5H_{1,1}(x_t). \quad (68)
\end{aligned}$$

The elements of the NNLO soft matrix in Laplace space are

$$\begin{aligned}
\tilde{s}_{gg11}^{(2)} &= \frac{31564}{27} - \frac{10504}{9}L + \frac{1742}{3}L^2 - \frac{286}{3}L^3 + \frac{338}{3}L^4 - \frac{4264}{81}N_l + \frac{1456}{27}LN_l - \frac{260}{9}L^2N_l \\
& + \frac{52}{9}L^3N_l + \frac{871}{18}\pi^2 + \frac{104}{9}\pi^2L^2 - \frac{65}{27}\pi^2N_l - \frac{461}{54}\pi^4 + 96L^2H_2(x_t) + 96L^2H_{0,0}(x_t) \\
& + 96L^2H_{1,0}(x_t) + 96L^2H_{1,1}(x_t) + 16\pi^2LH_0(x_t) + 16\pi^2LH_1(x_t) - 96LH_3(x_t) \\
& - 96LH_{1,2}(x_t) + 96LH_{2,0}(x_t) - 288LH_{2,1}(x_t) + 288LH_{0,0,0}(x_t) + 288LH_{1,0,0}(x_t) \\
& + 96LH_{1,1,0}(x_t) - 288LH_{1,1,1}(x_t) - 16\pi^2H_2(x_t) - 288H_4(x_t) + 16\pi^2H_{0,0}(x_t) \\
& + 16\pi^2H_{1,0}(x_t) - 16\pi^2H_{1,1}(x_t) - 288H_{1,3}(x_t) - 96H_{2,2}(x_t) - 96H_{3,0}(x_t) \\
& + 96H_{3,1}(x_t) - 96H_{1,1,2}(x_t) - 96H_{1,2,0}(x_t) + 96H_{1,2,1}(x_t) + 96H_{2,0,0}(x_t) - 288H_{2,1,0}(x_t) \\
& + 288H_{2,1,1}(x_t) + 288H_{0,0,0,0}(x_t) + 288H_{1,0,0,0}(x_t) + 96H_{1,1,0,0}(x_t) - 288H_{1,1,1,0}(x_t) \\
& + 288H_{1,1,1,1}(x_t) + 1092L\zeta(3) + \frac{52}{9}N_l\zeta(3) - \frac{286}{3}\zeta(3),
\end{aligned}$$

$$\begin{aligned}
\tilde{s}_{gg12}^{(2)} &= \frac{134}{3}\pi^2 + \frac{52}{3}\pi^2L^2 + \frac{4}{3}\pi^2LN_l - 22\pi^2L - \frac{20}{9}\pi^2N_l - \frac{68}{45}\pi^4 + \left[ 104L^3 + 4L^2N_l - 66L^2 \right. \\
&\quad \left. - \frac{40}{3}LN_l + \frac{52}{3}\pi^2L + 268L + \frac{4}{3}\pi^2N_l + \frac{112}{9}N_l + 252\zeta(3) - 22\pi^2 - \frac{808}{3} \right] H_0(x_t) \\
&\quad + \left[ 104L^3 + 4L^2N_l - 66L^2 - \frac{40}{3}LN_l + \frac{16}{3}\pi^2L + 268L + \frac{112}{9}N_l + \frac{4}{3}\pi^2N_l + 324\zeta(3) \right. \\
&\quad \left. - 22\pi^2 - \frac{808}{3} \right] H_1(x_t) + \left[ -104L^2 - 8LN_l + 132L + \frac{40}{3}N_l - \frac{16}{3}\pi^2 - 268 \right] H_2(x_t) \\
&\quad + \left[ 176L^2 + 8LN_l - 132L - \frac{40}{3}N_l + \frac{52}{3}\pi^2 + 268 \right] H_{0,0}(x_t) + \left[ 104L^2 + 8LN_l - 132L \right. \\
&\quad \left. - \frac{40}{3}N_l + \frac{16}{3}\pi^2 + 268 \right] H_{1,0}(x_t) + \left[ -176L^2 - 8LN_l + 132L + \frac{40}{3}N_l - \frac{52}{3}\pi^2 \right. \\
&\quad \left. - 268 \right] H_{1,1}(x_t) + \left[ 72L + 8N_l - 132 \right] H_{1,2}(x_t) + \left[ 72L + 8N_l - 132 \right] H_{2,0}(x_t) + \left[ 144L \right. \\
&\quad \left. + 8N_l - 132 \right] H_{2,1}(x_t) + \left[ 216L + 8N_l - 132 \right] H_{0,0,0}(x_t) + \left[ 144L + 8N_l - 132 \right] H_{1,0,0}(x_t) \\
&\quad + \left[ 216L + 8N_l - 132 \right] H_{1,1,1}(x_t) + \left[ 8N_l - 132 \right] H_3(x_t) + \left[ 8N_l - 132 \right] H_{1,1,0}(x_t) \\
&\quad + 72H_4(x_t) + 72H_{3,0}(x_t) - 72H_{1,1,2}(x_t) - 144H_{1,2,1}(x_t) + 144H_{2,0,0}(x_t) \\
&\quad - 72H_{2,1,1}(x_t) + 216H_{0,0,0,0}(x_t) + 72H_{1,0,0,0}(x_t) - 72H_{1,1,1,0}(x_t) - 216H_{1,1,1,1}(x_t) , \\
\tilde{s}_{gg13}^{(2)} &= \frac{5\pi^4}{9} + \frac{20}{3}\pi^2L \left[ H_0(x_t) + H_1(x_t) \right] + \left[ 40L^2 - \frac{20}{3}\pi^2 \right] \left[ H_2(x_t) + H_{1,1}(x_t) \right] \\
&\quad + \left[ 40L^2 + \frac{20}{3}\pi^2 \right] \left[ H_{0,0}(x_t) + H_{1,0}(x_t) \right] - 40LH_3(x_t) - 40LH_{1,2}(x_t) + 40LH_{2,0}(x_t) \\
&\quad - 120LH_{2,1}(x_t) + 120LH_{0,0,0}(x_t) + 120LH_{1,0,0}(x_t) + 40LH_{1,1,0}(x_t) - 120LH_{1,1,1}(x_t) \\
&\quad - 120H_4(x_t) - 120H_{1,3}(x_t) - 40H_{2,2}(x_t) - 40H_{3,0}(x_t) + 40H_{3,1}(x_t) - 40H_{1,1,2}(x_t) \\
&\quad - 40H_{1,2,0}(x_t) + 40H_{1,2,1}(x_t) + 40H_{2,0,0}(x_t) - 120H_{2,1,0}(x_t) + 120H_{2,1,1}(x_t) \\
&\quad + 120H_{0,0,0,0}(x_t) + 120H_{1,0,0,0}(x_t) + 40H_{1,1,0,0}(x_t) - 120H_{1,1,1,0}(x_t) + 120H_{1,1,1,1}(x_t) ,
\end{aligned}$$

$$\begin{aligned}
\tilde{s}_{99\ 22}^{(2)} = & \frac{15782}{27} - \frac{5252}{9}L + \frac{871}{3}L^2 - \frac{143}{3}L^3 + \frac{169}{3}L^4 - \frac{2132}{81}N_l + \frac{728}{27}N_lL - \frac{130}{9}N_lL^2 \\
& + \frac{26}{9}N_lL^3 + \frac{2077}{36}\pi^2 - \frac{33}{2}\pi^2L + \frac{169}{9}\pi^2L^2 - \frac{155}{54}N_l\pi^2 + N_l\pi^2L - \frac{673}{135}\pi^4 + \left[ 78L^3 \right. \\
& + 3N_lL^2 - \frac{99}{2}L^2 - 10N_lL + 26\pi^2L + 201L + N_l\pi^2 - \frac{33}{2}\pi^2 - 202 + \frac{28}{3}N_l \\
& \left. + 189\zeta(3) \right] H_0(x_t) + \left[ -78L^3 - 3N_lL^2 + \frac{99}{2}L^2 + 10N_lL - 201L - \frac{28}{3}N_l + N_l\pi^2 \right. \\
& \left. - \frac{33}{2}\pi^2 + 202 - 135\zeta(3) \right] H_1(x_t) + \left[ 102L^2 + 6N_lL - 99L - 10N_l + 201 \right] H_2(x_t) \\
& + \left[ 210L^2 + 6N_lL - 99L - 10N_l + 26\pi^2 + 201 \right] H_{0,0}(x_t) + \left[ 102L^2 + 6N_lL - 99L \right. \\
& \left. - 10N_l + 17\pi^2 + 201 \right] H_{1,0}(x_t) + \left[ 210L^2 + 6N_lL - 99L - 10N_l - 9\pi^2 + 201 \right] H_{1,1}(x_t) \\
& + \left[ -24L - 6N_l + 99 \right] H_3(x_t) + \left[ -132L - 6N_l + 99 \right] H_{1,2}(x_t) + \left[ -288L - 6N_l \right. \\
& \left. + 99 \right] H_{2,1}(x_t) + \left[ 132L + 6N_l - 99 \right] H_{2,0}(x_t) + \left[ 396L + 6N_l - 99 \right] H_{0,0,0}(x_t) \\
& + \left[ 288L + 6N_l - 99 \right] H_{1,0,0}(x_t) + \left[ 24L + 6N_l - 99 \right] H_{1,1,0}(x_t) + \left[ -396L - 6N_l \right. \\
& \left. + 99 \right] H_{1,1,1}(x_t) - 126H_4(x_t) - 72H_{1,3}(x_t) + 30H_{2,2}(x_t) + 84H_{3,0}(x_t) + 132H_{3,1}(x_t) \\
& + 84H_{1,1,2}(x_t) + 30H_{1,2,0}(x_t) + 240H_{1,2,1}(x_t) + 240H_{2,0,0}(x_t) - 72H_{2,1,0}(x_t) + 288H_{2,1,1}(x_t) \\
& + 396H_{0,0,0,0}(x_t) + 288H_{1,0,0,0}(x_t) + 132H_{1,1,0,0}(x_t) - 126H_{1,1,1,0}(x_t) + 396H_{1,1,1,1}(x_t) \\
& - \frac{143}{3}\zeta(3) + \frac{26}{9}N_l\zeta(3) + 546\zeta(3)L,
\end{aligned}$$

$$\begin{aligned}
\tilde{s}_{99\ 23}^{(2)} = & \frac{335}{18}\pi^2 - \frac{55}{6}\pi^2L + \frac{65}{9}\pi^2L^2 - \frac{25}{27}N_l\pi^2 + \frac{5}{9}N_l\pi^2L - \frac{23}{108}\pi^4 + \left[ \frac{130}{3}L^3 + \frac{5}{3}N_lL^2 - \frac{55}{2}L^2 \right. \\
& \left. - \frac{50}{9}N_lL + \frac{110}{9}\pi^2L + \frac{335}{3}L + \frac{140}{27}N_l + \frac{5}{9}N_l\pi^2 - \frac{55}{6}\pi^2 - \frac{1010}{9} + 105\zeta(3) \right] H_0(x_t) \\
& + \left[ \frac{130}{3}L^3 + \frac{5}{3}N_lL^2 - \frac{55}{2}L^2 - \frac{50}{9}N_lL + \frac{20}{9}\pi^2L + \frac{335}{3}L + \frac{140}{27}N_l + \frac{5}{9}N_l\pi^2 - \frac{55}{6}\pi^2 - \frac{1010}{9} \right.
\end{aligned}$$

$$\begin{aligned}
& + 135\zeta(3) \Big] H_1(x_t) + \left[ -\frac{130}{3}L^2 - \frac{10}{3}N_lL + 55L + \frac{50}{9}N_l - \frac{20}{9}\pi^2 - \frac{335}{3} \right] H_2(x_t) + \left[ \frac{310}{3}L^2 \right. \\
& + \frac{10}{3}N_lL - 55L + \frac{110}{9}\pi^2 + \frac{335}{3} - \frac{50}{9}N_l \Big] H_{0,0}(x_t) + \left[ \frac{130}{3}L^2 - 55L + \frac{10}{3}N_lL - \frac{50}{9}N_l \right. \\
& + \frac{65}{9}\pi^2 + \frac{335}{3} \Big] H_{1,0}(x_t) + \left[ -\frac{310}{3}L^2 - \frac{10}{3}N_lL + 55L + \frac{50}{9}N_l - \frac{65}{9}\pi^2 - \frac{335}{3} \right] H_{1,1}(x_t) \\
& + \left[ 60L + \frac{10}{3}N_l - 55 \right] \left[ H_{1,2}(x_t) + H_{2,0}(x_t) \right] + \left[ 120L + \frac{10}{3}N_l - 55 \right] H_{2,1}(x_t) + \left[ 180L \right. \\
& + \frac{10}{3}N_l - 55 \Big] \left[ H_{0,0,0}(x_t) + H_{1,1,1}(x_t) \right] + \left[ 120L + \frac{10}{3}N_l - 55 \right] H_{1,0,0}(x_t) + \left[ \frac{10}{3}N_l \right. \\
& - 55 \Big] H_3(x_t) + 30H_4(x_t) - 30H_{2,2}(x_t) + 60H_{3,0}(x_t) - 60H_{3,1}(x_t) + \frac{10}{3}N_lH_{1,1,0}(x_t) \\
& - 55H_{1,1,0}(x_t) - 60H_{1,1,2}(x_t) + 30H_{1,2,0}(x_t) - 120H_{1,2,1}(x_t) + 120H_{2,0,0}(x_t) \\
& - 120H_{2,1,1}(x_t) + 180H_{0,0,0,0}(x_t) + 120H_{1,0,0,0}(x_t) + 60H_{1,1,0,0}(x_t) - 30H_{1,1,1,0}(x_t) \\
& - 180H_{1,1,1,1}(x_t) . \\
\tilde{s}_{gg}^{(2)33} & = \frac{78910}{243} - \frac{26260}{81}L + \frac{4355}{27}L^2 - \frac{715}{27}L^3 + \frac{845}{27}L^4 - \frac{10660}{729}N_l + \frac{3640}{243}N_lL - \frac{650}{81}N_lL^2 \\
& + \frac{130}{81}N_lL^3 + \frac{10385}{324}\pi^2 - \frac{55}{6}\pi^2L + \frac{845}{81}\pi^2L^2 - \frac{775}{486}N_l\pi^2 + \frac{5}{9}N_l\pi^2L - \frac{763}{243}\pi^4 + \left[ \frac{130}{3}L^3 \right. \\
& + \frac{5}{3}N_lL^2 - \frac{55}{2}L^2 + \frac{335}{3}L - \frac{50}{9}N_lL + 10\pi^2L + \frac{5}{9}N_l\pi^2 - \frac{55}{6}\pi^2 - \frac{1010}{9} + \frac{140}{27}N_l \\
& + 105\zeta(3) \Big] H_0(x_t) + \left[ -\frac{130}{3}L^3 - \frac{5}{3}N_lL^2 + \frac{55}{2}L^2 + \frac{50}{9}N_lL - \frac{40}{9}\pi^2L - \frac{335}{3}L + \frac{5}{9}N_l\pi^2 \right. \\
& - \frac{55}{6}\pi^2 + \frac{1010}{9} - \frac{140}{27}N_l - 75\zeta(3) \Big] H_1(x_t) + \left[ 30L^2 + \frac{10}{3}N_lL - 55L - \frac{50}{9}N_l + \frac{40}{9}\pi^2 \right. \\
& + \frac{335}{3} \Big] H_2(x_t) + \left[ 90L^2 + \frac{10}{3}N_lL - 55L - \frac{50}{9}N_l + 10\pi^2 + \frac{335}{3} \right] H_{0,0}(x_t) + \left[ 30L^2 \right.
\end{aligned}$$

$$\begin{aligned}
& + \frac{10}{3}N_l L - 55L - \frac{50}{9}N_l + 5\pi^2 + \frac{335}{3} \Big] H_{1,0}(x_t) + \left[ 90L^2 + \frac{10}{3}N_l L - 55L - \frac{50}{9}N_l - \frac{5}{9}\pi^2 \right. \\
& + \left. \frac{335}{3} \right] H_{1,1}(x_t) + \left[ \frac{40}{3}L - \frac{10}{3}N_l + 55 \right] H_3(x_t) + \left[ \frac{140}{3}L + \frac{10}{3}N_l - 55 \right] \left[ H_{2,0}(x_t) \right. \\
& - \left. H_{1,2}(x_t) \right] + \left[ -80L - \frac{10}{3}N_l + 55 \right] H_{2,1}(x_t) + \left[ 140L + \frac{10}{3}N_l - 55 \right] \left[ H_{0,0,0}(x_t) \right. \\
& - \left. H_{1,1,1}(x_t) \right] + \left[ 80L + \frac{10}{3}N_l - 55 \right] H_{1,0,0}(x_t) + \left[ -\frac{40}{3}L - 55 \right] H_{1,1,0}(x_t) + 10H_4(x_t) \\
& + 40H_{1,3}(x_t) + \frac{130}{3}H_{2,2}(x_t) + \frac{220}{3}H_{3,0}(x_t) + \frac{140}{3}H_{3,1}(x_t) + \frac{10}{3}N_l H_{1,1,0}(x_t) \\
& + \frac{220}{3}H_{1,1,2}(x_t) + \frac{130}{3}H_{1,2,0}(x_t) + \frac{320}{3}H_{1,2,1}(x_t) + \frac{320}{3}H_{2,0,0}(x_t) + 40H_{2,1,0}(x_t) \\
& + 80H_{2,1,1}(x_t) + 140H_{0,0,0,0}(x_t) + 80H_{1,0,0,0}(x_t) + \frac{140}{3}H_{1,1,0,0}(x_t) + 10H_{1,1,1,0}(x_t) \\
& + 140H_{1,1,1,1}(x_t) + \frac{130N_l\zeta(3)}{81} - \frac{715}{27}\zeta(3) + \frac{910L}{3}\zeta(3). \tag{69}
\end{aligned}$$

## References

- [1] M. L. Mangano, P. Nason and G. Ridolfi, Nucl. Phys. B **373**, 295 (1992).
- [2] N. Kidonakis and G. F. Sterman, Nucl. Phys. B **505**, 321 (1997) [hep-ph/9705234].
- [3] L. G. Almeida, G. F. Sterman and W. Vogelsang, Phys. Rev. D **78**, 014008 (2008) [arXiv:0805.1885 [hep-ph]].
- [4] V. Ahrens, A. Ferroglia, M. Neubert, B. D. Pecjak and L. L. Yang, JHEP **1009**, 097 (2010) [arXiv:1003.5827 [hep-ph]].
- [5] D. Appell, G. F. Sterman and P. B. Mackenzie, Nucl. Phys. B **309**, 259 (1988).
- [6] S. Catani, M. L. Mangano and P. Nason, JHEP **9807**, 024 (1998) [hep-ph/9806484].
- [7] T. Becher, M. Neubert and G. Xu, JHEP **0807**, 030 (2008) [arXiv:0710.0680 [hep-ph]].
- [8] C. W. Bauer, N. D. Dunn and A. Hornig, arXiv:1010.0243 [hep-ph].
- [9] V. Ahrens, A. Ferroglia, M. Neubert, B. D. Pecjak and L. L. Yang, Phys. Lett. B **687**, 331 (2010) [arXiv:0912.3375 [hep-ph]].

- [10] P. Baernreuther, M. Czakon and A. Mitov, arXiv:1204.5201 [hep-ph].
- [11] M. Czakon and A. Mitov, arXiv:1207.0236 [hep-ph].
- [12] A. Ferroglia, B. D. Pecjak and L. L. Yang, arXiv:1205.3662 [hep-ph].
- [13] K. Melnikov and A. Mitov, Phys. Rev. D **70**, 034027 (2004) [hep-ph/0404143].
- [14] C. Anastasiou, E. W. N. Glover, C. Oleari and M. E. Tejeda-Yeomans, Nucl. Phys. B **601**, 318 (2001) [hep-ph/0010212].
- [15] C. Anastasiou, E. W. N. Glover, C. Oleari and M. E. Tejeda-Yeomans, Phys. Lett. B **506**, 59 (2001) [hep-ph/0012007].
- [16] E. W. N. Glover, C. Oleari and M. E. Tejeda-Yeomans, Nucl. Phys. B **605**, 467 (2001) [hep-ph/0102201].
- [17] E. W. N. Glover and M. E. Tejeda-Yeomans, JHEP **0105**, 010 (2001) [hep-ph/0104178].
- [18] C. Anastasiou, E. W. N. Glover, C. Oleari and M. E. Tejeda-Yeomans, Nucl. Phys. B **605**, 486 (2001) [hep-ph/0101304].
- [19] A. V. Belitsky, Phys. Lett. B **442**, 307 (1998) [hep-ph/9808389].
- [20] T. Becher and M. Neubert, Phys. Lett. B **633**, 739 (2006) [hep-ph/0512208].
- [21] R. Kelley, M. D. Schwartz, R. M. Schabinger and H. X. Zhu, Phys. Rev. D **84**, 045022 (2011) [arXiv:1105.3676 [hep-ph]].
- [22] P. F. Monni, T. Gehrmann and G. Luisoni, JHEP **1108**, 010 (2011) [arXiv:1105.4560 [hep-ph]].
- [23] A. Hornig, C. Lee, I. W. Stewart, J. R. Walsh and S. Zuberi, JHEP **1108**, 054 (2011) [arXiv:1105.4628 [hep-ph]].
- [24] Y. Li, S. Mantry and F. Petriello, Phys. Rev. D **84**, 094014 (2011) [arXiv:1105.5171 [hep-ph]].
- [25] R. Kelley, M. D. Schwartz, R. M. Schabinger and H. X. Zhu, arXiv:1112.3343 [hep-ph].
- [26] T. Becher, G. Bell and S. Marti, JHEP **1204**, 034 (2012) [arXiv:1201.5572 [hep-ph]].
- [27] J. G. M. Gatheral, Phys. Lett. B **133**, 90 (1983).
- [28] J. Frenkel and J. C. Taylor, Nucl. Phys. B **246**, 231 (1984).
- [29] S. M. Aybat, L. J. Dixon and G. F. Sterman, Phys. Rev. Lett. **97**, 072001 (2006) [hep-ph/0606254].
- [30] S. M. Aybat, L. J. Dixon and G. F. Sterman, Phys. Rev. D **74**, 074004 (2006) [hep-ph/0607309].

- [31] T. Becher and M. Neubert, Phys. Rev. Lett. **102**, 162001 (2009) [arXiv:0901.0722 [hep-ph]].
- [32] E. Gardi and L. Magnea, JHEP **0903**, 079 (2009) [arXiv:0901.1091 [hep-ph]].
- [33] T. Becher and M. Neubert, JHEP **0906**, 081 (2009) [arXiv:0903.1126 [hep-ph]].
- [34] S. Catani and M. H. Seymour, Phys. Lett. B **378**, 287 (1996) [hep-ph/9602277].
- [35] S. Catani and M. H. Seymour, Nucl. Phys. B **485**, 291 (1997) [Erratum-ibid. B **510**, 503 (1998)] [hep-ph/9605323].
- [36] W. L. van Neerven, Nucl. Phys. B **268**, 453 (1986).
- [37] E. Remiddi and J. A. M. Vermaseren, Int. J. Mod. Phys. A **15**, 725 (2000) [hep-ph/9905237].
- [38] T. Huber and D. Maitre, Comput. Phys. Commun. **175**, 122 (2006) [hep-ph/0507094].
- [39] D. Maitre, Comput. Phys. Commun. **174**, 222 (2006) [hep-ph/0507152].
- [40] A. Ferroglia, M. Neubert, B. D. Pecjak and L. L. Yang, Phys. Rev. Lett. **103**, 201601 (2009) [arXiv:0907.4791 [hep-ph]].
- [41] A. Ferroglia, M. Neubert, B. D. Pecjak and L. L. Yang, JHEP **0911**, 062 (2009) [arXiv:0908.3676 [hep-ph]].
- [42] N. Kidonakis, Phys. Rev. D **82**, 114030 (2010) [arXiv:1009.4935 [hep-ph]].
- [43] V. Ahrens, A. Ferroglia, M. Neubert, B. D. Pecjak and L. -L. Yang, JHEP **1109**, 070 (2011) [arXiv:1103.0550 [hep-ph]].